

Sensor and Simulation Notes  
Note XLIV  
15 June 1967

The Capacitor Driven, Open Circuited, Buried-  
Transmission-Line Simulator

Capt Carl E. Baum  
Air Force Weapons Laboratory

Abstract

The buried transmission line is combined with a capacitive energy source and a series resistance. The resulting pulse shapes for the electromagnetic fields are calculated using numerical inverse Fourier transforms. The pulse shapes are calculated over a wide range of the various values for the capacitor, series resistor, and parameters describing the transmission line.

*PLPA 10/27/94*

Sensor and Simulation Notes  
Note XLIV  
15 June 1967

The Capacitor Driven, Open Circuited, Buried-  
Transmission-Line Simulator

Capt Carl E. Baum  
Air Force Weapons Laboratory

Abstract

The buried transmission line is combined with a capacitive energy source and a series resistance. The resulting pulse shapes for the electromagnetic fields are calculated using numerical inverse Fourier transforms. The pulse shapes are calculated over a wide range of the various values for the capacitor, series resistor, and parameters describing the transmission line.

## Foreword

The pulse shapes fall into two convenient cases depending on whether or not the finite length of the transmission line is included in the calculations. The figures for each case are grouped together at the end of the two sections of concern.

We would like to thank Mr. Robert Myers for most of the numerical calculations and graphs, together with some assistance from AIC Franklin Brewster, Mr. Ronald Thompson, and Mr. John N. Wood.

## Contents

<u>Section</u>	<u>Page</u>
I Introduction	4
II Effectively Infinite-Length Transmission Line	6
Figures 2-8	13
III Finite-Length, Open Circuited Transmission Line	20
Figures 9-25	24
IV Some Low-Frequency Considerations	41
V Summary	43

## I. Introduction

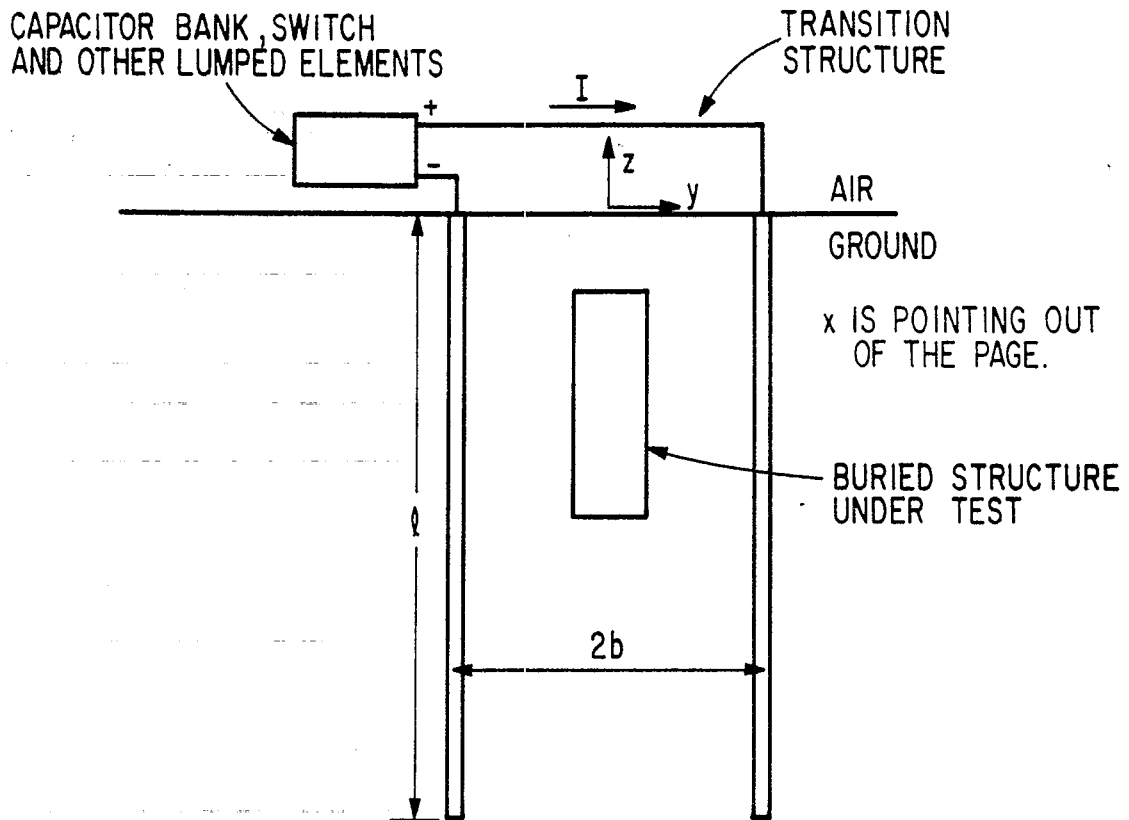
In a previous note we discussed a simulation technique which might be called the buried transmission line.<sup>1</sup> The buried transmission line consists of a set of parallel conductors placed in the earth such that, when electrically driven from the top end, a TEM wave propagates along the structure into the ground. This TEM wave is attenuated in much the same fashion as the nuclear electromagnetic pulse as it propagates into the earth. One limitation of the buried transmission line is its finite length. Practically the bottom end of the transmission line would not be terminated in its frequency-dependent characteristic impedance; typically the bottom end would be left in an open-circuited configuration. The wave then reflects from the bottom of the transmission line, somewhat distorting the ideal distribution of the electromagnetic fields with depth along the transmission line. This last type of field distortion can be reduced by increasing the depth,  $z$ , to which the transmission line extends.

Typically a buried transmission line might consist of two parallel grids of conducting rods in good electrical contact with the earth. Each grid might approximate a conducting plate of width,  $2a$ , with the two grids separated by a distance,  $2b$ . Then if  $a/b$  is about one or larger the field distribution between the two grids is roughly uniform at a given depth, thereby approximating a homogeneous plane wave. For the response of the buried transmission line we only consider frequencies low enough that wavelengths above the ground surface are much larger than the cross section dimensions,  $2a$  and  $2b$ . The length,  $l$ , is also assumed much larger than  $2a$  and  $2b$  so that the distortion of the ideal field distributions near the ends of the line can be neglected. With an appropriate transition structure connecting the electrical energy sources to the top of the transmission line, the field distortion at the top can be minimized. However, it may be impractical to do anything similar at the bottom of the transmission line.

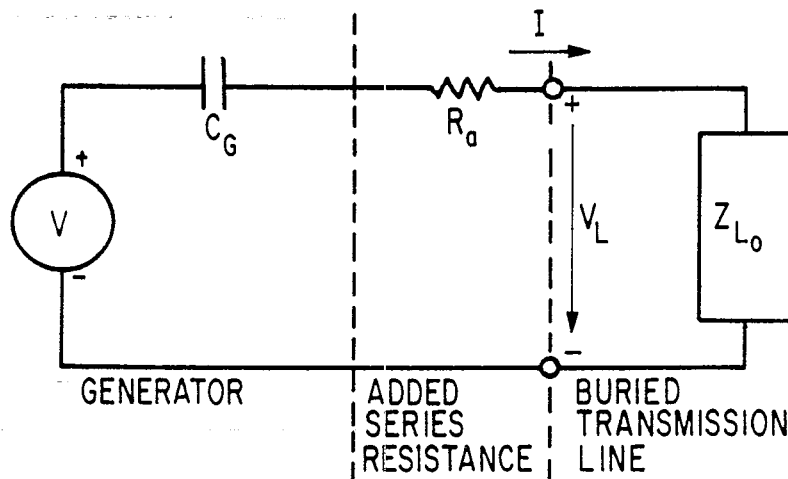
In the previous note we considered the dependence of the transmission-line impedance on frequency and the dependence of field distribution on frequency and depth. Then the dependence of the field distribution on time and depth was calculated for a step function driving current. Thus the previous note considered the response functions of the buried transmission line. In this note we consider the pulse shapes produced by a capacitive energy source with a series damping resistance when driving a buried transmission line. The assumptions used in the previous note are carried over to this note. The conductivity,  $\sigma$ , is assumed independent of depth and frequency,  $\omega$ . The permittivity,  $\epsilon$ , is neglected because the frequencies of interest are assumed low enough that  $\sigma \gg \omega\epsilon$ .

---

1. Lt Carl E. Baum, Sensor and Simulation Note XXII, A Transmission Line EMP Simulation Technique for Buried Structures, June 1966.



A. SIDE VIEW



B. EQUIVALENT CIRCUIT

FIGURE 1. BURIED TRANSMISSION LINE WITH CAPACITIVE ENERGY SOURCE AND SERIES RESISTANCE

Figure 1 illustrates the buried transmission line and its equivalent circuit, including the generator of capacitance,  $C_G$ , charged to a voltage,  $V_G$ . A switch is closed, defining the time,  $t=0$ . The capacitor is discharged through an added series resistance of value,  $R_a$ , into the buried transmission line of impedance,  $Z_{L_0}$ . In the equivalent circuit the switch is replaced by a voltage generator of value

$$V = V_G u(t) \quad (1)$$

where  $u(t)$  is the unit step function, rising to one at  $t=0$ . Note that no resistance or inductance in the generator and/or transition structure is included in the analysis, except that resistance which one might include with  $R_a$ . A capacitive generator is a common electrical energy source; the resistor is added to give some flexibility in shaping the pulse. There are various other energy sources and pulse shaping elements one might consider but these are not included in this note.

The buried transmission line is only considered with the bottom in the open-circuited configuration. The calculation of the pulse shapes falls into two convenient cases. First, the length of the transmission line is so long that for times and depths of interest the finite length has little significant effect on the pulse. The length is thus assumed to be infinite, simplifying the results somewhat. Second, the times of interest are comparable to or greater than the diffusion time characteristic of the length of the transmission line, and/or the depths of interest are close enough to the bottom of the transmission line for the pulse to be significantly influenced by the reflection from the bottom. The finite length of the transmission line is then included in the calculations. In each of these cases the Laplace transform of the pulse shape is developed in normalized form. Converting these to Fourier transforms a computer program is used to numerically obtain the time domain wave forms.<sup>2</sup> After considering the time domain wave forms we go on to some low-frequency considerations regarding the time integrals of the pulse shapes: for such limited cases the variation of the soil conductivity with depth can be easily included in the calculations.

## II. Effectively Infinite Length Transmission Line

Consider first the case that  $l$  is sufficiently large that we may consider it infinite as far as its effect on the pulse shape for times of interest is concerned. The current,  $I$ , into the transmission line is related to  $V$  as<sup>3</sup>

$$\tilde{I}(s) = \tilde{V}(s) \left[ Z_{L_\infty} + R_a + \frac{1}{sC_G} \right]^{-1} \quad (2)$$

---

2. Frank Sulkowski, Mathematics Note II, FORPLEX: A Program to Calculate Inverse Fourier Transforms, November 1966.

3. All units are rationalized MKSA.

where the tilde,  $\tilde{\phantom{V}}$ , over a quantity indicated the Laplace transform of the quantity, and where  $Z_{L\infty}$  is used for the impedance of the effectively infinite length transmission line. Substituting for  $Z_{L\infty}$  from reference 1 and for  $\tilde{V}(s)$  from equation (1) gives

$$\tilde{I}(s) = V_G C_G \left[ s^{3/2} C_G f_g \sqrt{\frac{\mu}{\sigma}} + s R_a C_G + 1 \right]^{-1} \quad (3)$$

where  $f_g$  is a dimensionless geometrical factor for the transmission line which is multiplied by the wave impedance of the ground to give the impedance of the transmission line.

For convenience, we define characteristic times as

$$t_c \equiv \left[ C_G^2 f_g^2 \frac{\mu}{\sigma} \right]^{1/3} \quad (4)$$

$$t_a \equiv R_a C_G \quad (5)$$

and

$$t_z \equiv \frac{\mu \sigma z^2}{4} \quad (6)$$

where  $-z$  is the depth into the ground. (Note that  $z$  is a negative number of meters.) Then define a normalized Laplace transform variable as

$$s_c \equiv s t_c \quad (7)$$

Inverting such normalized Laplace transforms into the time domain, the results are expressed in terms of a normalized time which we define as

$$\tau_c \equiv \frac{t}{t_c} \quad (8)$$

A characteristic current is also defined as

$$I_c \equiv \frac{V_G C_G}{t_c} \quad (9)$$

With these various definitions the form of the results simplifies somewhat.

Dividing  $\tilde{I}(s)$  by  $t_c$  we then have a normalized Laplace transform of the current into the transmission line from equation (3) as

$$\tilde{i}_c(s_c) \equiv \frac{\tilde{I}(s)}{t_c} = I_c \left[ s_c^{3/2} + s_c \frac{t_a}{t_c} + 1 \right]^{-1} \quad (10)$$

It is necessary to divide by  $t_c$  because for the inverse Fourier transform the integral is performed over  $\omega$  which is set equal to  $-j s_c$  which equals  $-j s t_c$ . A similar procedure is followed for other normalized Laplace transforms elsewhere in this note. Having the current at the top of the transmission line, then multiply this by  $e^{\sqrt{s \mu \sigma} z}$  to obtain the current on the transmission line as a function of depth.

Multiplying this current by a factor determined by the cross section dimensions of the transmission line and the position of interest on the cross section gives the magnetic field at the position of interest. Then define a normalized current or magnetic field as

$$\tilde{h}_c(s_c) \equiv \frac{\tilde{i}_c(s_c)}{I_c} e^{\sqrt{s\mu\sigma}z} = e^{-2\sqrt{s_c} \frac{t_z}{t_c}} \left[ s_c^{3/2} + s_c \frac{t_a}{t_c} + 1 \right]^{-1} \quad (11)$$

Inverting this into the time domain gives  $h_c(\tau_c)$  which one can multiply by  $I_c$  to give the current on the transmission line conductors at a particular  $z$  (negative). Multiplying in turn by a factor appropriate to the particular geometry and dimensions of the cross section (independent of depth) of the transmission line gives the magnetic field.

The voltage,  $V_L$ , at the top of the transmission line is given by

$$\tilde{V}_L(s) = Z_{L\infty} \tilde{I}(s) \quad (12)$$

Substituting for  $I(s)$  from equation (3) gives

$$\tilde{V}_L(s) = f \sqrt{\frac{s\mu}{\sigma}} V_G C_G \left[ s^{3/2} C_G f \sqrt{\frac{\mu}{\sigma}} + s R_a C_G + 1 \right]^{-1} \quad (13)$$

Converting to normalized form we have the Laplace transform of the voltage at the top of the transmission line as

$$\tilde{v}_c(s_c) \equiv \frac{\tilde{V}_L(s)}{t_c} = V_G \sqrt{s_c} \left[ s_c^{3/2} + s_c \frac{t_a}{t_c} + 1 \right]^{-1} \quad (14)$$

Divide by  $V_G$  and multiply by  $e^{\sqrt{s\mu\sigma}z}$  to define a normalized voltage or electric field or current density as

$$\tilde{e}_c(s_c) \equiv \frac{\tilde{v}_c(s_c)}{V_G} e^{\sqrt{s\mu\sigma}z} = \sqrt{s_c} e^{-2\sqrt{s_c} \frac{t_z}{t_c}} \left[ s_c^{3/2} + s_c \frac{t_a}{t_c} + 1 \right]^{-1} \quad (15)$$

Inverting this into the time domain gives  $e_c(\tau_c)$  which one can multiply by  $V_G$  to give the voltage across the transmission line at a particular  $z$ . This can in turn be related to the electric field or current density in the ground through the particular geometry and dimensions of the cross section of the transmission line.

Consider first the pulse shapes at the ground surface as plotted in Figure 2. Note that for  $R_a=0$  (making  $t_a/t_c = 0$ ) both  $h_c$  and  $e_c$  ring, damping out in a few cycles. The magnetic field has a maximum of  $h_{c_{max}} \approx .726$  and a minimum of  $h_{c_{min}} \approx -.148$ . As  $t_a/t_c$  is increased from zero the wave forms are damped and  $h_{c_{max}}$  is decreased. At  $t_a/t_c \approx 1$  the undershoot of  $h_c$  is rather small compared to the initial peak; such a pulse might be roughly considered as critically damped. In Figure 3 the maximum and minimum values of  $h_c$  as well as the times of the maximum ( $t_{max}$ ),

minimum ( $t_{min}$ ), and first crossover ( $t_{cr}$ ) are plotted versus  $t_a/t_c$ . There is an asymptotic form for  $h_{cmax}$  which applies for large  $t_a/t_c$  which one can obtain from equation (11) by setting  $t_z=0$  and neglecting  $s_c^{3/2}$  compared to  $s_c t_a/t_c$ . This gives

$$\tilde{h}_c(s_c) \Big|_{\frac{t_z}{t_c} = 0} \sim \frac{1}{s_c \frac{t_a}{t_c} + 1} \quad (16)$$

which in the time domain is

$$\tilde{h}_c(\tau_c) \Big|_{\frac{t_z}{t_c} = 0} \sim \frac{t_c}{t_a} e^{-\frac{t_c}{t_a} \tau_c} = \frac{t_c}{t_a} e^{-\frac{t}{t_a}} \quad (17)$$

From this the maximum value is approximately

$$h_{cmax} \sim \frac{t_c}{t_a} \quad (18)$$

This asymptotic form is included in Figure 3A.

Figures 4 through 6 have the variation of the pulse shapes with depth into the ground for three values of  $t_a/t_c$ . Note that as  $t_z/t_c$  is increased both  $h_c$  and  $e_c$  decrease in amplitude and spread out in time. Looking at Figure 4 for which  $t_a/t_c = 0$ , note that increasing  $t_z/t_c$  also decreases the ringing of the pulse shapes. In Figure 7 the maximum value of  $h_c$  and the time of the maximum is plotted versus  $t_z/t_c$  for four values of  $t_a/t_c$ . Note that  $h_{cmax}$  decreases with increasing depth ( $-z$ ) and that  $t_{max}$  increases with increasing depth. There are asymptotic forms for  $h_{cmax}$  and  $t_{max}$  which apply for large  $t_z/t_c$  which one can obtain from equation (11) by neglecting both  $s_c^{3/2}$  and  $s_c t_a/t_c$  compared to one. This gives

$$\tilde{h}_c(s_c) \sim e^{-2\sqrt{s_c} \frac{t_z}{t_c}} \quad (19)$$

which in the time domain is

$$h_c(\tau_c) \sim \sqrt{\frac{t_z}{\pi t_c \tau_c^3}} e^{-\frac{t_z}{t_c \tau_c}} = \frac{t_c}{\sqrt{\pi t_z}} \left( \frac{t_z}{t} \right)^{3/2} e^{-\frac{t_z}{t}} \quad (20)$$

To determine the peak of this function set the time derivative to zero, giving

$$0 \sim \frac{t_c}{\sqrt{\pi t_z}} \left[ -\frac{3}{2} \left( \frac{t_z}{t_{max}} \right)^{5/2} e^{-\frac{t_z}{t_{max}}} + \left( \frac{t_z}{t_{max}} \right)^{7/2} e^{-\frac{t_z}{t_{max}}} \right] \quad (21)$$

which has the solution  $\frac{t_{\max}}{t_z} \sim \frac{2}{3}$  (22)

or  $\frac{t_{\max}}{t_c} \sim \frac{2}{3} \frac{t_z}{t_c}$  (23)

Substituting this into equation (20) gives

$$h_{c\max} \sim \frac{t_c}{t_z \sqrt{\pi}} \left( \frac{3}{2} \right)^{\frac{3}{2}} e^{-\frac{3}{2}} \sim .231 \frac{t_c}{t_z} \quad (24)$$

Equations (24) and (23) are included as asymptotic forms in Figures 7A and 7B, respectively.

Now consider the limiting case of large  $C_G$ . Setting  $C_G \rightarrow \infty$  makes the current from equation (2) become

$$\tilde{I}(s) = \frac{V_G}{R_a s} \left[ \frac{f_g \sqrt{s\mu} + 1}{R_a} \right]^{-1} \quad (25)$$

Then define

$$t'_a \equiv \left( \frac{f_g}{R_a} \right)^2 \frac{\mu}{\sigma} \quad (26)$$

$$s'_a \equiv s t'_a \quad (28)$$

$$\tau'_a \equiv \frac{t_c}{t_a} \quad (28)$$

and  $I'_a \equiv \frac{V_G}{R_a}$  (29)

The normalized Laplace transform of the current into the transmission line is then

$$\tilde{i}'_a(s'_a) \equiv \frac{\tilde{I}(s)}{t_a} = I'_a \left[ s'_a (\sqrt{s'_a} + 1) \right]^{-1} \quad (30)$$

Multiply this by  $e^{\sqrt{s\mu\sigma} z}$  and divide by  $I'_a$  to obtain a normalized current or magnetic field as a function of depth, giving

$$\tilde{h}'(s'_a) \equiv \frac{\tilde{i}'_a(s'_a) e^{\sqrt{s\mu\sigma} z}}{I'_a} = e^{-2\sqrt{s'_a} \frac{t_z}{t'_a}} \left[ s'_a (\sqrt{s'_a} + 1) \right]^{-1} \quad (31)$$

This normalized Laplace transform can be inverted to give<sup>4</sup>

$$h_a'(\tau_a') = -e^{2\sqrt{\frac{t_z}{t_a'} + \tau_a'}} \operatorname{erfc}\left(\sqrt{\tau_a'} + \sqrt{\frac{t_z}{t_a'\tau_a'}}\right) + \operatorname{erfc}\left(\sqrt{\frac{t_z}{t_a'\tau_a'}}\right) \quad (32)$$

For the special case of  $z=0$  this reduces to

$$h_a'(\tau_a') \Big|_{\frac{t_z}{t_a'} = 0} = 1 - e^{\tau_a'} \operatorname{erfc}(\sqrt{\tau_a'}) \quad (33)$$

In this form one multiplies  $h_a'$  by  $I_a'$  to obtain the current on the transmission line.

The voltage at the top of the transmission line from equation (12) for  $C_G = \infty$  becomes

$$\tilde{V}_L(s) = \frac{V_G}{R_a s} f_g \sqrt{\frac{s\mu}{\sigma}} \left[ \frac{f_g}{R_a} \sqrt{\frac{s\mu}{\sigma}} + 1 \right]^{-1} \quad (34)$$

The normalized Laplace transform of the voltage at the top of the transmission line is then

$$\tilde{v}_a'(s_a') \equiv \frac{\tilde{V}_L(s)}{t_a'} = V_G \left[ \sqrt{s_a'} (\sqrt{s_a'} + 1) \right]^{-1} \quad (35)$$

Multiply this by  $e^{\sqrt{s\mu\sigma} z}$  and divide by  $V_G$  to obtain a normalized voltage or electric field or current density as a function of depth as

$$e_a'(s_a') \equiv \frac{\tilde{v}_a'(s_a')}{V_G} e^{\sqrt{s\mu\sigma} z} = e^{-2\sqrt{s_a'} \frac{t_z}{t_a'}} \left[ \sqrt{s_a'} (\sqrt{s_a'} + 1) \right]^{-1} \quad (36)$$

Changing to the time domain

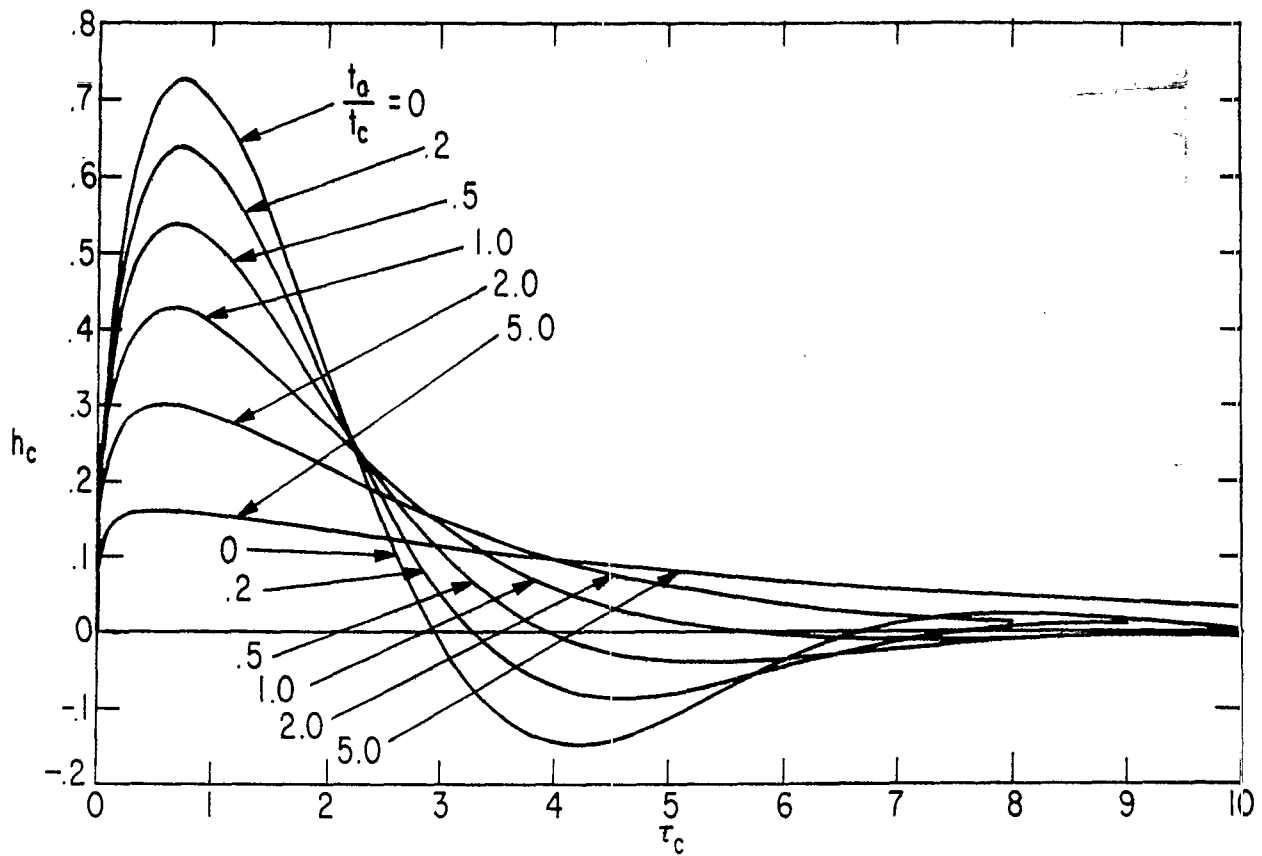
$$e_a'(\tau_a') \equiv e^{2\sqrt{\frac{t_z}{t_a'} + \tau_a'}} \operatorname{erfc}\left(\sqrt{\tau_a'} + \sqrt{\frac{t_z}{t_a'\tau_a'}}\right) \quad (37)$$

which for  $z=0$  reduces to

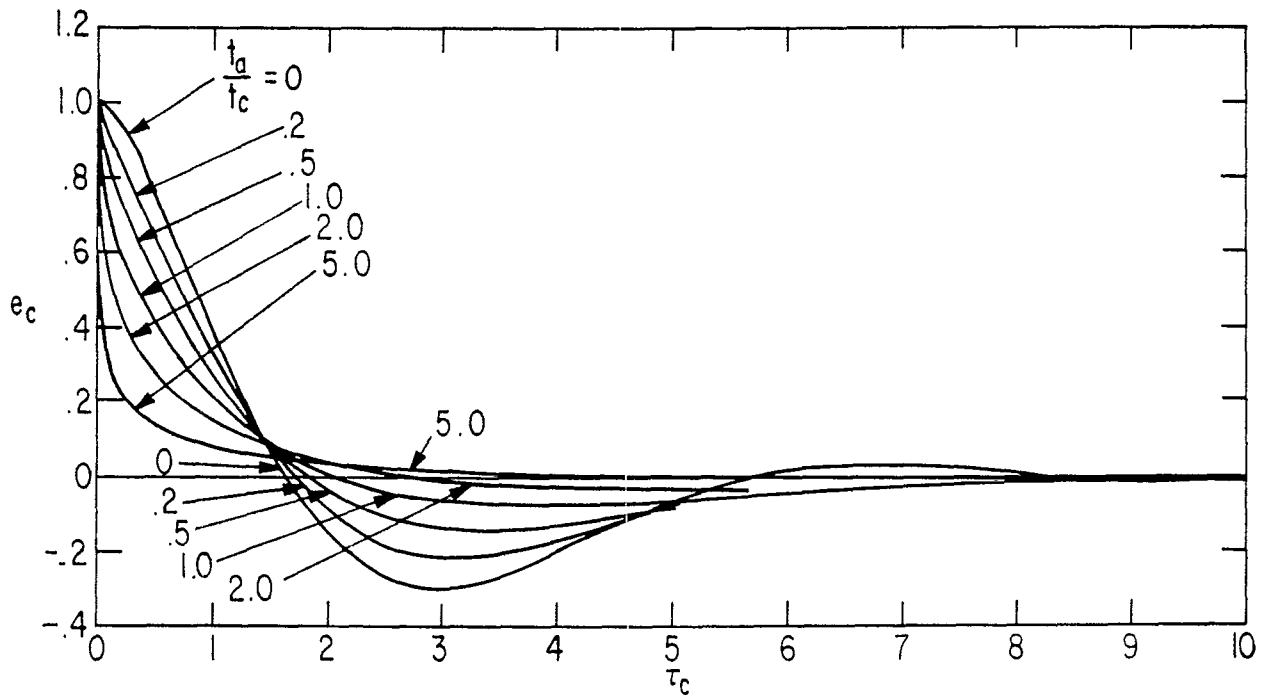
$$e_a'(\tau_a') \Big|_{\frac{t_z}{t_a'} = 0} = e^{\tau_a'} \operatorname{erfc}(\sqrt{\tau_a'}) \quad (38)$$

4. See AMS 55, Handbook of Mathematical Functions, National Bureau of Standards, 1964, for the inverse Laplace transforms.

The results of equations (32) and (37) are plotted in Figures 8A and 8B, respectively. Note that as  $t_2/t_a'$  is increased the rise of the pulse shapes is slowed down. This limiting case of large  $C_G$  may sometimes be useful in describing the initial rise of the waveforms for times for which the capacitor has not appreciably discharged.

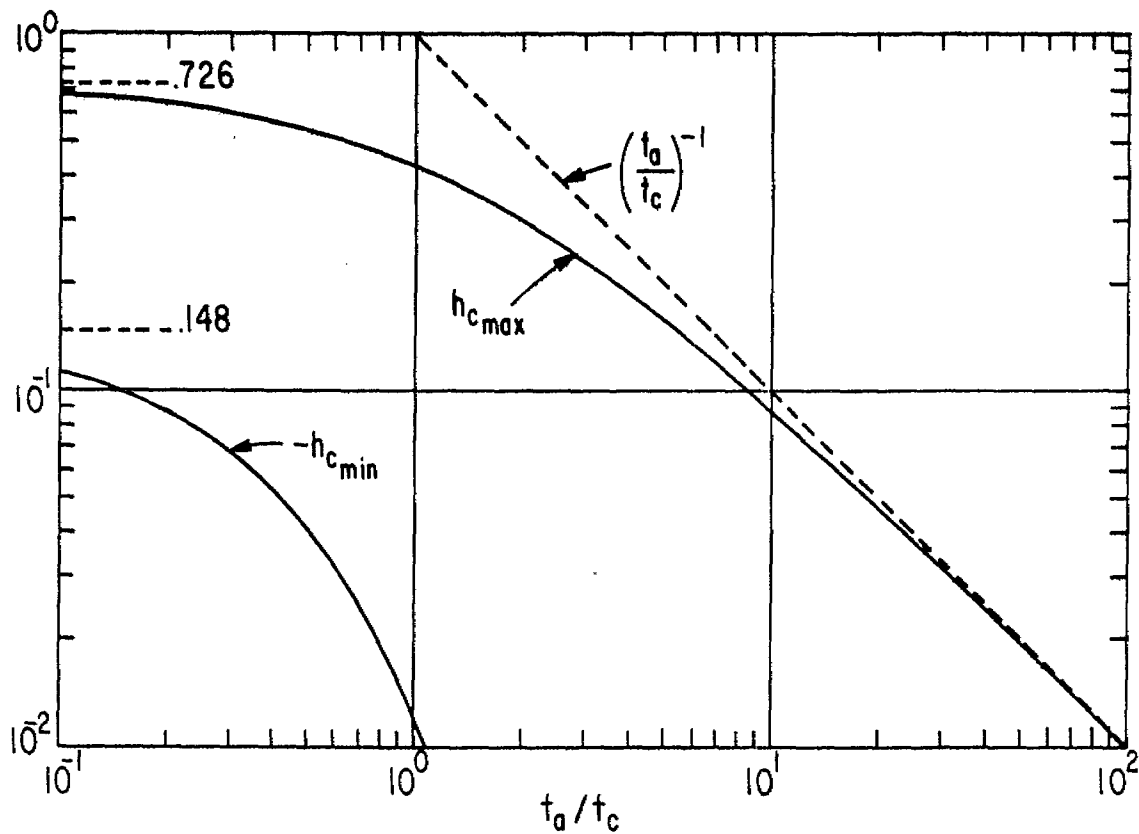


A.  $h_c$  vs  $\tau_c$  WITH  $t_a/t_c$  AS A PARAMETER

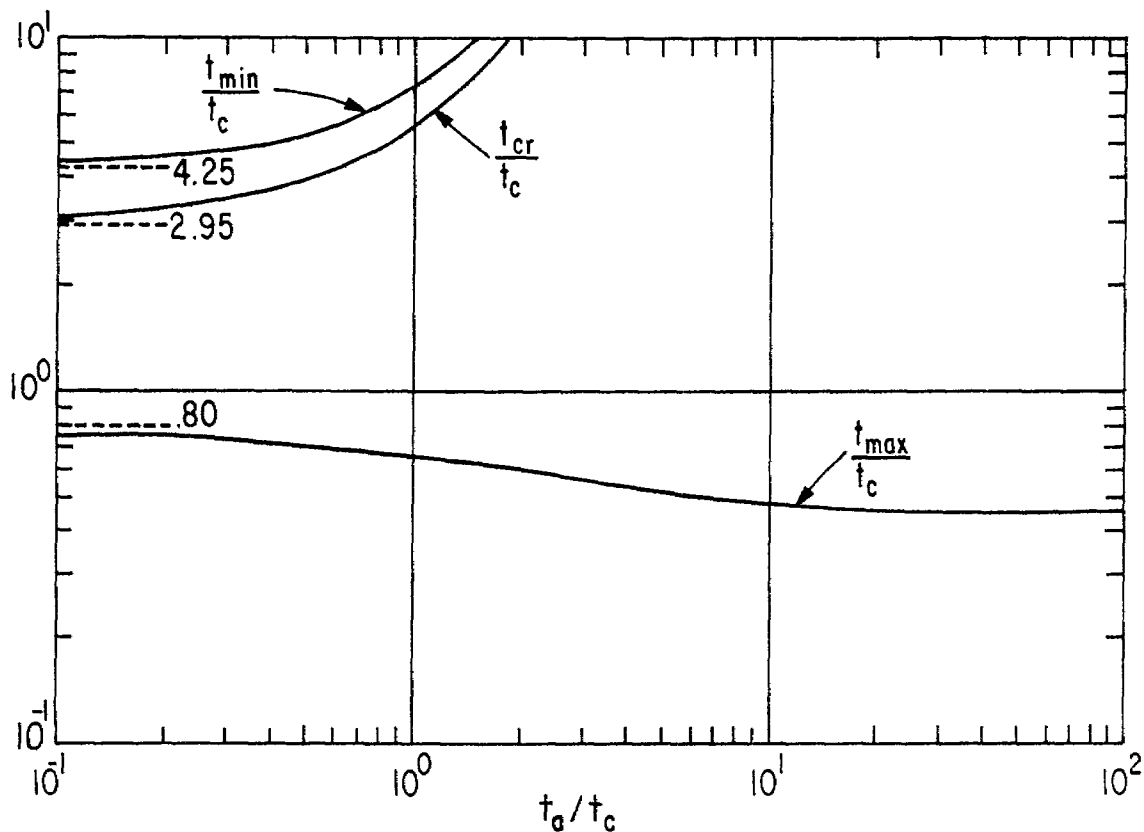


B.  $e_c$  vs  $\tau_c$  WITH  $t_a/t_c$  AS A PARAMETER

FIGURE 2. PULSE SHAPES AT GROUND SURFACE FOR INFINITE LENGTH TRANSMISSION LINE:  $t_z/t_c = 0$

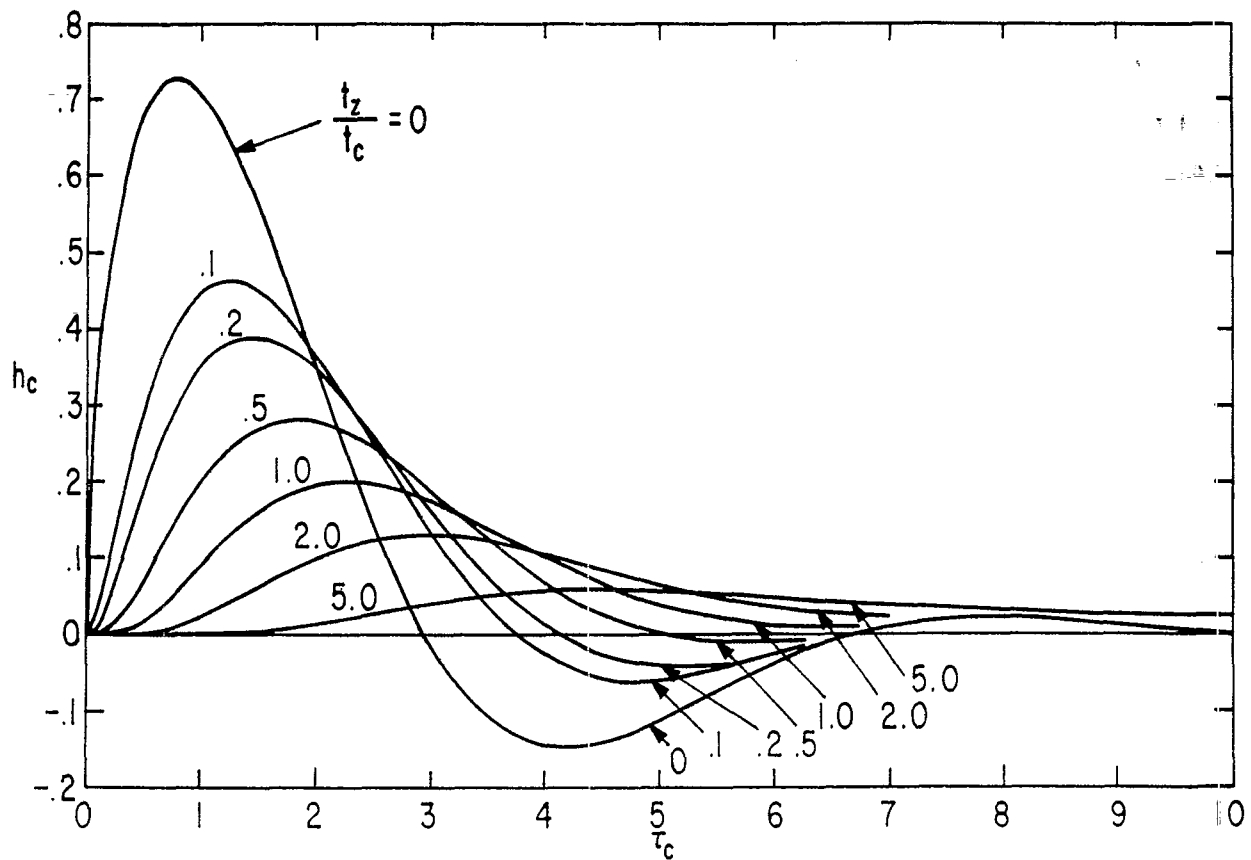


A. VALUES OF MAXIMUM AND MINIMUM vs  $t_a/t_c$

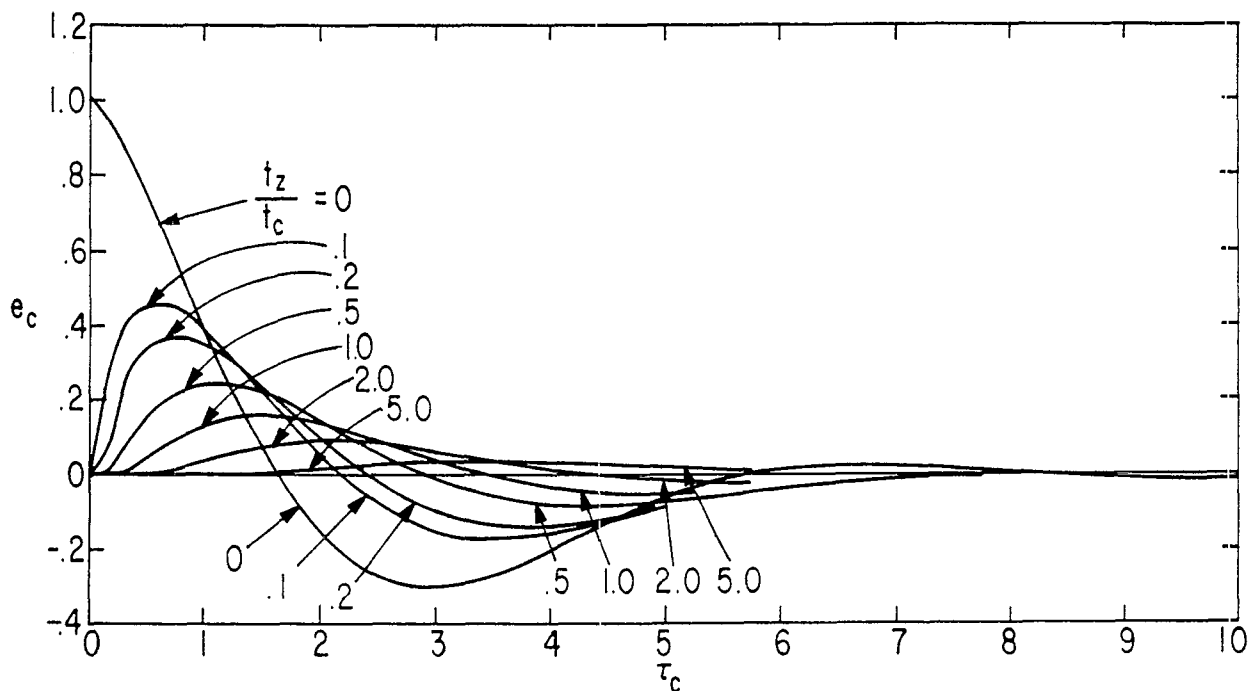


B. TIMES OF MAXIMUM, CROSSOVER, AND MINIMUM vs  $t_a/t_c$

FIGURE 3. PARAMETERS OF CURRENT OR MAGNETIC FIELD PULSE SHAPE AT GROUND SURFACE FOR INFINITE LENGTH TRANSMISSION LINE

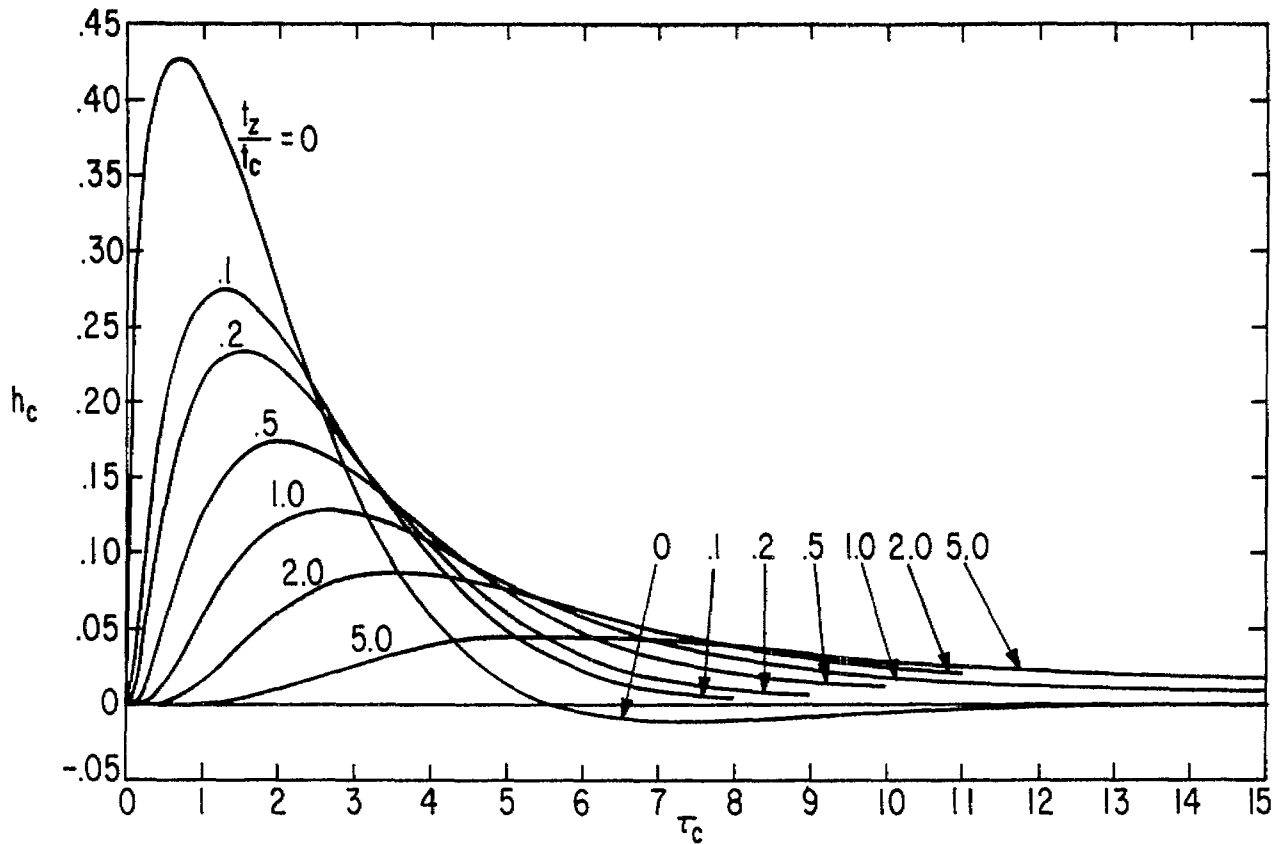


A.  $h_c$  vs  $\tau_c$  WITH  $t_z/t_c$  AS A PARAMETER

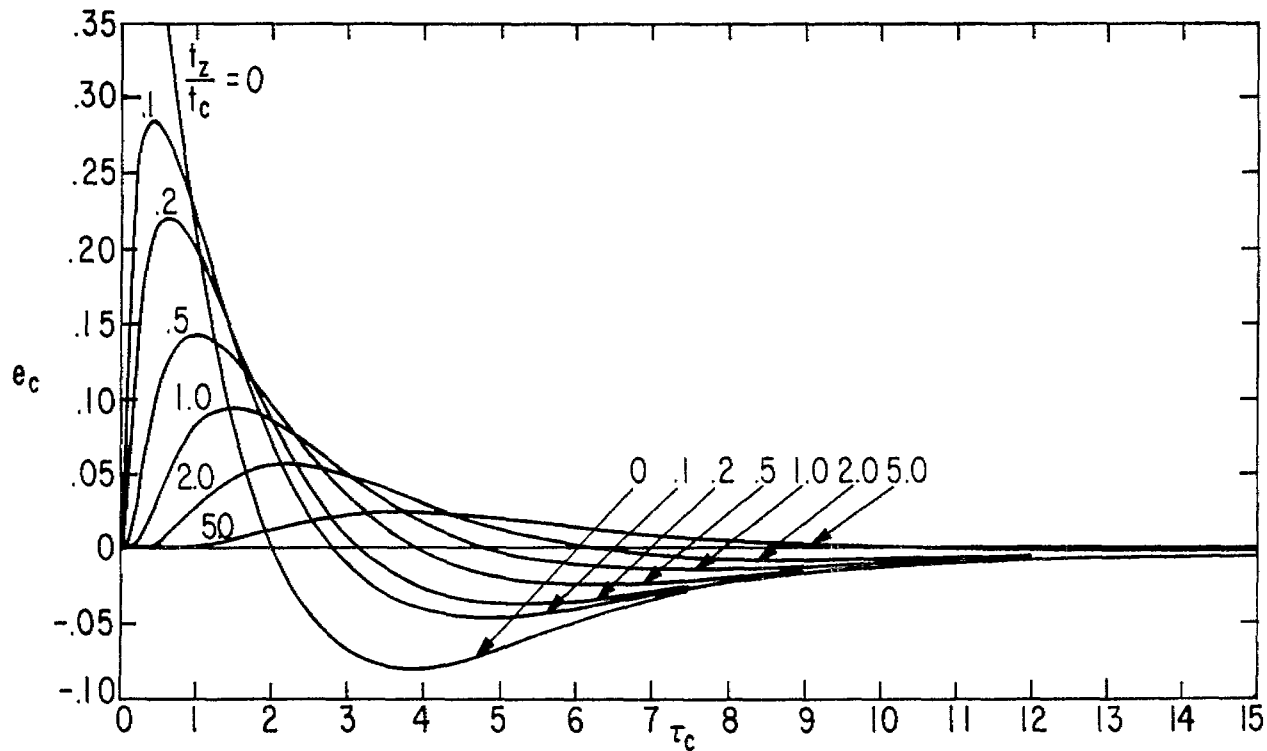


B.  $e_c$  vs  $\tau_c$  WITH  $t_z/t_c$  AS A PARAMETER

FIGURE 4. PULSE SHAPES IN GROUND FOR INFINITE LENGTH TRANSMISSION LINE:  $t_a/t_c = 0$

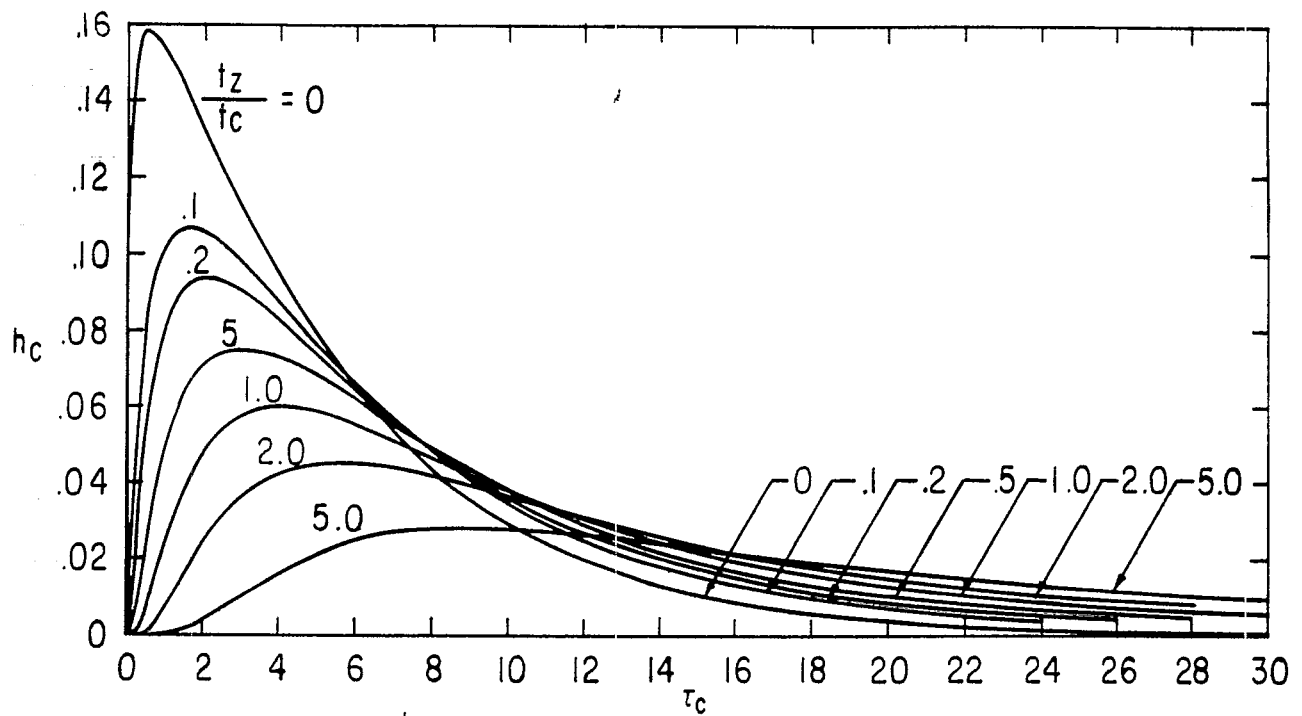


A.  $h_c$  vs  $\tau_c$  WITH  $t_z/t_c$  AS A PARAMETER

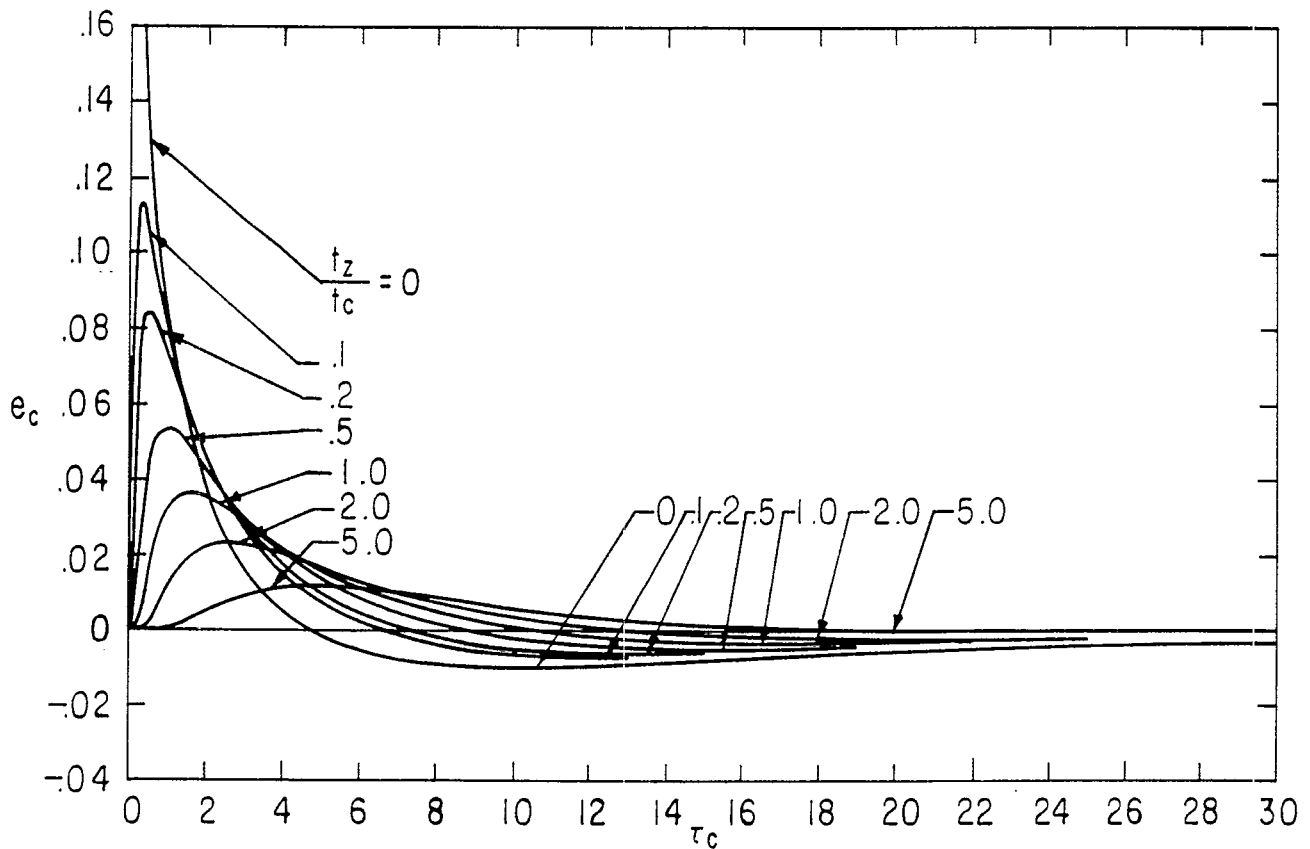


B.  $e_c$  vs  $\tau_c$  WITH  $t_z/t_c$  AS A PARAMETER

FIGURE 5. PULSE SHAPES IN GROUND FOR INFINITE LENGTH TRANSMISSION LINE:  $t_0/t_c = 1$

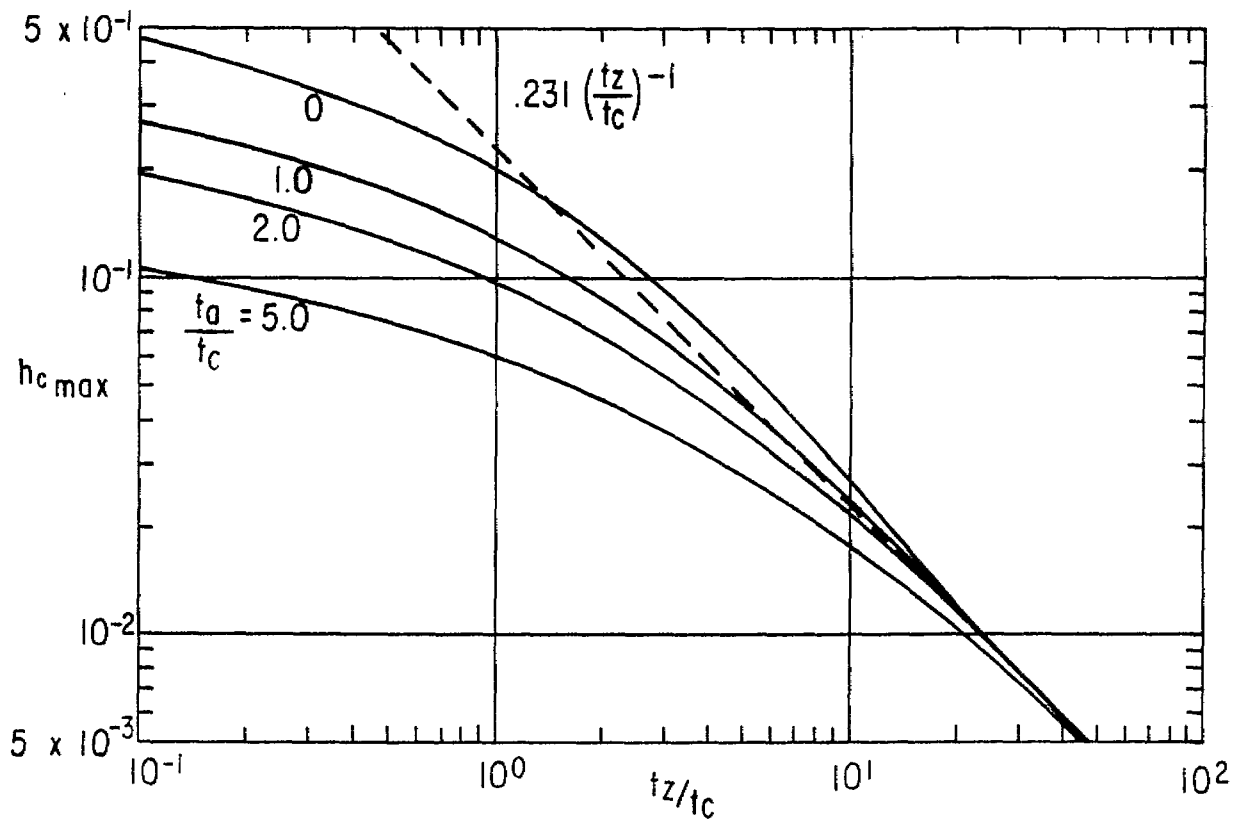


A.  $h_c$  vs  $\tau_c$  WITH  $t_z/t_c$  AS A PARAMETER

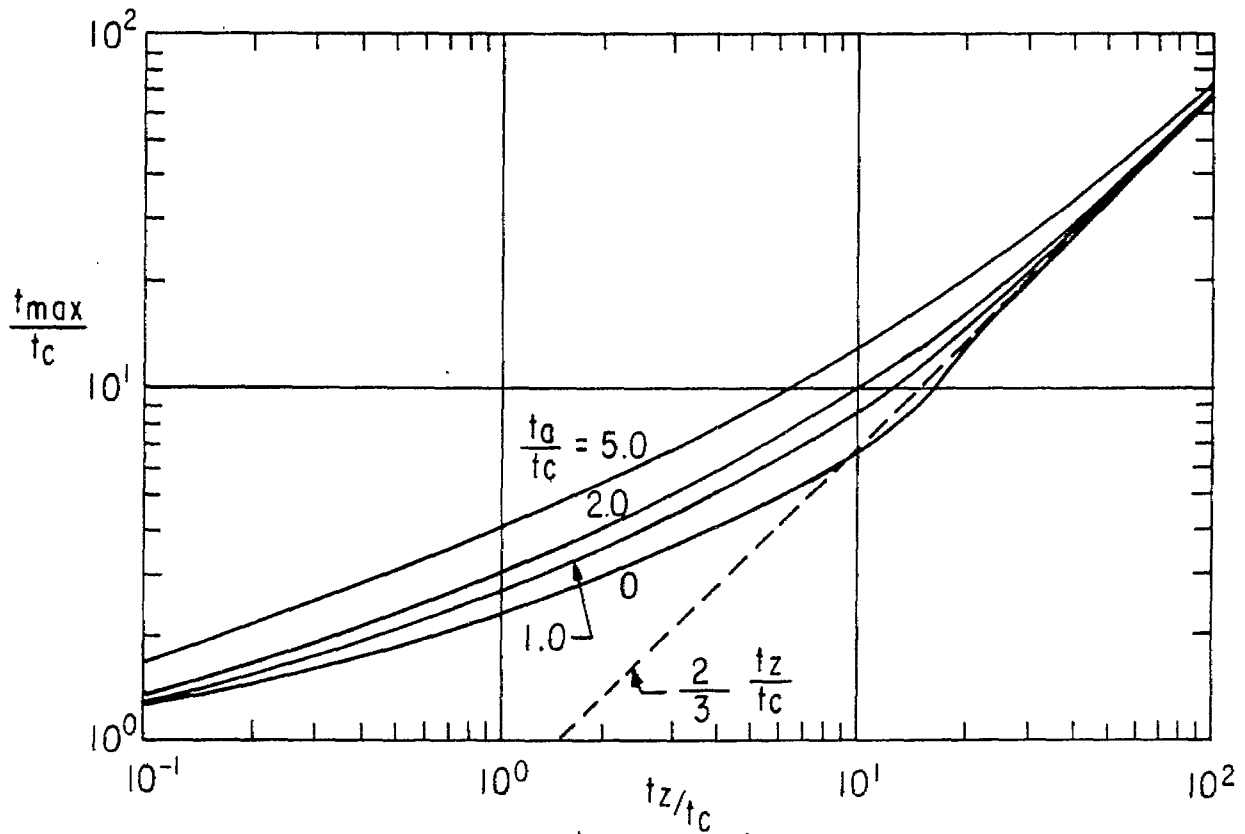


B.  $e_c$  vs  $\tau_c$  WITH  $t_z/t_c$  AS A PARAMETER

FIGURE 6. PULSE SHAPES IN GROUND FOR INFINITE LENGTH TRANSMISSION LINE:  $t_a/t_c = 5$



A. VALUE OF MAXIMUM vs  $t_z/t_c$  WITH  $t_a/t_c$  AS A PARAMETER



B. TIME OF MAXIMUM vs  $t_z/t_c$  WITH  $t_a/t_c$  AS A PARAMETER

FIGURE 7. PARAMETERS OF CURRENT OR MAGNETIC FIELD PULSE SHAPE vs DEPTH IN GROUND FOR INFINITE LENGTH TRANSMISSION LINE

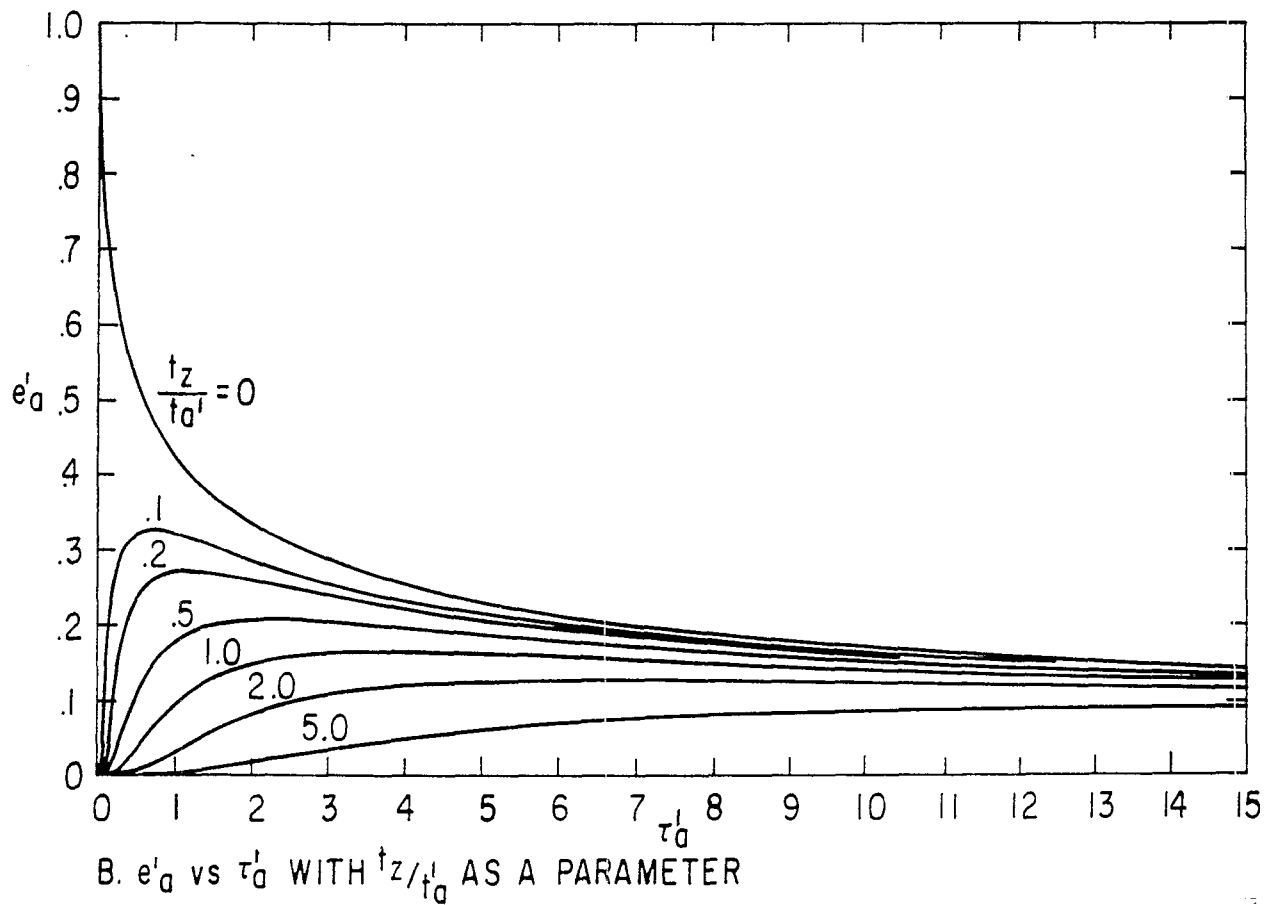
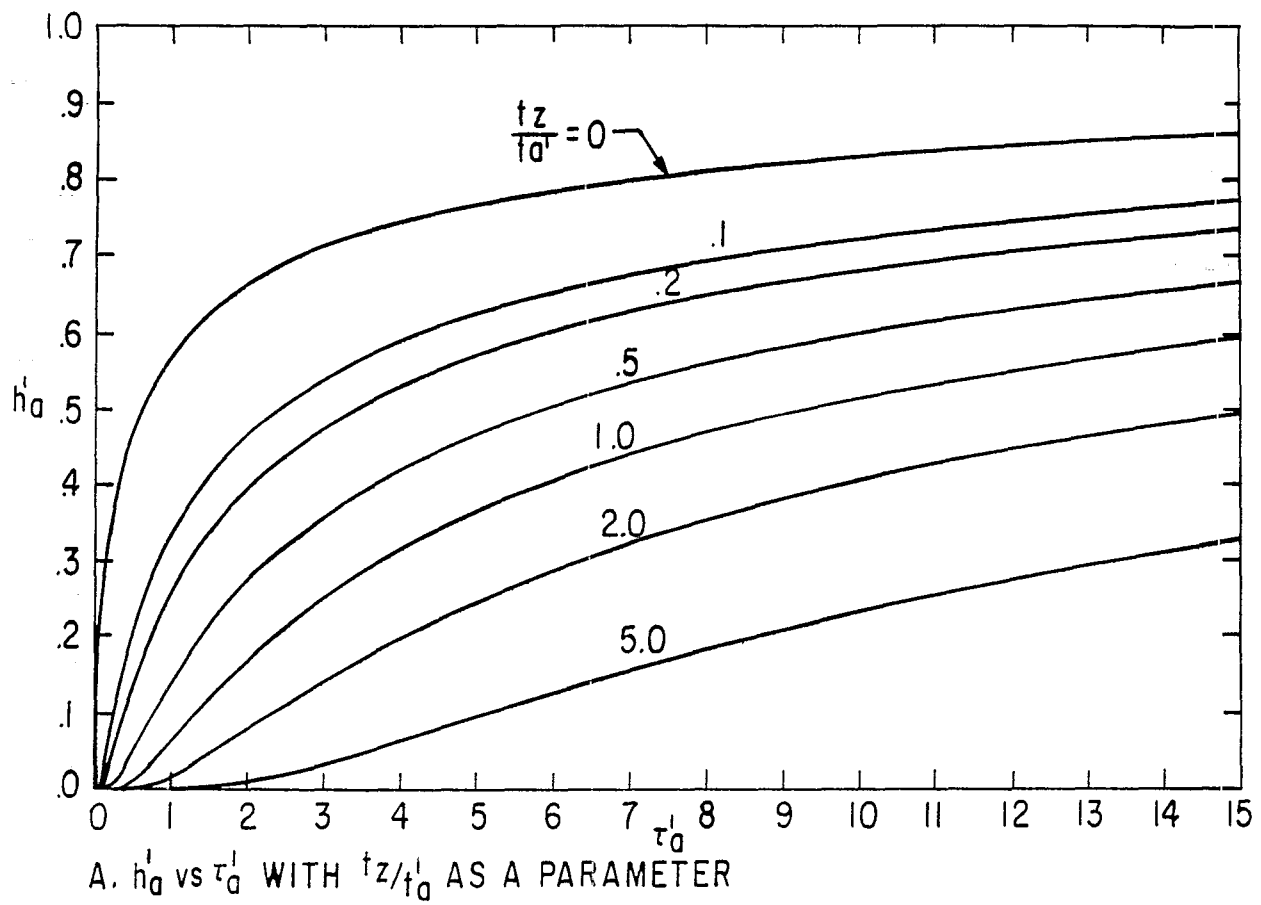


FIGURE 8. PULSE SHAPES IN GROUND FOR INFINITE LENGTH TRANSMISSION LINE AND INFINITE GENERATOR CAPACITANCE

### III. Finite-Length, Open Circuited Transmission Line

Now consider the case that reflections from the bottom of the transmission line are significant for times and/or depths of interest and are thus included in the calculations. The current into the transmission line is given by

$$\tilde{I}(s) = \frac{V_G}{s} \left[ Z_{L_0} + R_a + \frac{1}{sC_G} \right]^{-1} \quad (39)$$

The impedance of the transmission line is

$$Z_{L_0} = f_g \sqrt{\frac{s\mu}{\sigma}} \frac{1 + e^{-2\sqrt{s\mu\sigma} \ell}}{1 - e^{-2\sqrt{s\mu\sigma} \ell}} = R_0 \sqrt{s\mu\sigma} \ell \frac{1 + e^{-2\sqrt{s\mu\sigma} \ell}}{1 - e^{-2\sqrt{s\mu\sigma} \ell}} \quad (40)$$

where, as in reference 1, we have defined

$$R_0 \equiv \frac{f_g}{\ell\sigma} \quad (41)$$

This last parameter is the resistance of the open-circuited transmission line at zero frequency.

Define some characteristic times as

$$t_\ell \equiv \frac{\mu\sigma\ell^2}{4} \quad (42)$$

and

$$t_0 \equiv R_0 C_G \quad (43)$$

We also use  $t_a$  as defined in equation (5). Define a normalized Laplace transform variable as

$$s_\ell \equiv s t_\ell \quad (44)$$

Inverting such normalized Laplace transforms, the results are expressed in terms of a normalized time defined as

$$\tau_\ell \equiv \frac{t}{t_\ell} \quad (45)$$

For the finite length transmission line the times are then based on a characteristic diffusion time,  $t_\ell$ , for the transmission line. (This same time base was used in reference 1.) Define also a characteristic current as

$$I_0 \equiv \frac{V_G}{R_0 + R_a} \quad (46)$$

and a normalized depth as

$$z' \equiv -\frac{z}{l} \quad (47)$$

Dividing  $\tilde{I}(s)$  by  $t_l$  gives the normalized Laplace transform of the current into the transmission line as

$$\tilde{i}_l(s_l) \equiv \frac{\tilde{I}(s)}{t_l} = I_0 \left[ 1 + \frac{R_a}{R_o} \right] \left\{ 2s_l^{\frac{3}{2}} \frac{1 + e^{-4\sqrt{s_l}l}}{1 - e^{-4\sqrt{s_l}l}} + s_l \frac{R_a}{R_o} + \frac{t_l}{t_o} \right\}^{-1} \quad (48)$$

To obtain a normalized current or magnetic field note first that the current or magnetic field has a -1 reflection at the bottom of the transmission line so that

$$\frac{\tilde{h}_l(s_l)}{\tilde{i}_l(s_l)} = \frac{e^{\sqrt{s_l}\mu\sigma z} - e^{-\sqrt{s_l}\mu\sigma(2l+z)}}{1 - e^{-2\sqrt{s_l}\mu\sigma l}} \quad (49)$$

Multiplying this by  $\tilde{i}_l(s_l)/I_0$  the normalized current or magnetic field is then defined as

$$\tilde{h}_l(s_l) \equiv \left[ \frac{1+R_a}{R_o} \right] \frac{e^{-2\sqrt{s_l}z'} - e^{-2\sqrt{s_l}(2-z')}}{1 - e^{-4\sqrt{s_l}l}} \left\{ 2s_l^{\frac{3}{2}} \frac{1 + e^{-4\sqrt{s_l}l}}{1 - e^{-4\sqrt{s_l}l}} + s_l \frac{R_a}{R_o} + \frac{t_l}{t_o} \right\}^{-1} \quad (50)$$

In another form this becomes

$$\tilde{h}_l(s_l) = \left[ \frac{1+t_a}{t_o} \right] \frac{e^{-2\sqrt{s_l}z'} - e^{-2\sqrt{s_l}(2-z')}}{1 - e^{-4\sqrt{s_l}l}} \left\{ 2s_l^{\frac{3}{2}} \frac{1 + e^{-4\sqrt{s_l}l}}{1 - e^{-4\sqrt{s_l}l}} + s_l \frac{t_a}{t_o} + \frac{t_l}{t_o} \right\}^{-1} \quad (51)$$

In the time domain multiply  $h_l(\tau_l)$  by  $I_0$  to give the current on the transmission line. Multiply this in turn by an appropriate factor to obtain the magnetic field.

As in reference 1 we define a normalized current density by relating it to the normalized magnetic field at the top of the transmission line as

$$l \tilde{j}_l(s_l) \equiv \tilde{h}_l(s_l) \left\{ \frac{e^{\sqrt{s_l}\mu\sigma z} - e^{-\sqrt{s_l}\mu\sigma(2l+z)}}{1 + e^{-2\sqrt{s_l}\mu\sigma l}} \frac{l\sigma}{f_g} Z_{L_0} \right\} \quad (52)$$

Note that the normalized current density has a +1 reflection at the bottom of the transmission line. Combining the results of equations (40) and (50) then gives

$$\tilde{h}_\ell(s_\ell) = \left[ \frac{1+R_a}{R_o} \right] 2\sqrt{s_\ell} \frac{e^{-2\sqrt{s_\ell}z'} + e^{-2\sqrt{s_\ell}(2-z')}}{1-e^{-4\sqrt{s_\ell}}} \left\{ 2s_\ell \frac{1+e^{-4\sqrt{s_\ell}}}{1-e^{-4\sqrt{s_\ell}}} + s_\ell \frac{R_a}{R_o} + \frac{t_\ell}{t_o} \right\}^{-1} \quad (53)$$

In another form this becomes

$$\tilde{h}_\ell(s_\ell) = \left[ \frac{1+t_a}{t_o} \right] 2\sqrt{s_\ell} \frac{e^{-2\sqrt{s_\ell}z'} + e^{-2\sqrt{s_\ell}(2-z')}}{1-e^{-4\sqrt{s_\ell}}} \left\{ 2s_\ell \frac{1+e^{-4\sqrt{s_\ell}}}{1-e^{-4\sqrt{s_\ell}}} + s_\ell \frac{t_a}{t_o} + \frac{t_\ell}{t_o} \right\}^{-1} \quad (54)$$

Note that this form of the normalized voltage or electric field or current density differs from that used in section II for the infinite length transmission line. To obtain the voltage on the transmission line multiply  $\tilde{h}_\ell(\tau_\ell)$  by a factor,  $I_o R_o$ , which also is of the form

$$I_o R_o = V_G \left[ \frac{1+R_a}{R_o} \right]^{-1} \quad (55)$$

The voltage on the transmission line can then still be obtained from  $\tilde{h}_\ell(\tau_\ell)$  with little difficulty; multiplying the voltage by an appropriate factor gives the electric field or current density in the ground. Note also that the initial rise of  $\tilde{h}_\ell(\tau_\ell)$  for  $z'=0$  is to a value

$$\tilde{h}_\ell(0+) \Big|_{z'=0} = \frac{1+t_a}{t_o} = \frac{1+R_a}{R_o} \quad (56)$$

Consider first the pulse shapes at the ground surface where  $z'=0$ . Starting with Figure 9, for which  $R_a$  is set to zero or equivalently  $t_a/t_\ell = 0$ , note that as  $t_o/t_\ell$  is increased the oscillation of the pulse shapes is reduced. At  $t_o/t_\ell \approx 3$  the pulse shapes might be roughly considered as critically damped. Then for  $t_o/t_\ell > 3$  one does not need to add resistance to dampen the pulse although one might still add resistance to broaden the pulse. Figures 10 and 11 include the effect of varying  $t_a/t_\ell$ . Each graph is for a particular value of  $t_o/t_\ell$  and each curve on a graph is for a particular value of  $t_a/t_\ell$ . Note that in the limit of  $t_o/t_\ell$  and  $t_a/t_\ell$  both small compared to one, the approximation of an infinite length transmission line becomes more and more appropriate and the calculations of section II apply. If either  $t_o/t_\ell$  or  $t_a/t_\ell$  is large compared to one the pulse shape broadens out; there are no oscillations and the decay of the pulse is roughly exponential. To approximate the decay of the magnetic field for  $t_o$  and/or  $t_a$  much larger than  $t_\ell$ , expand the exponentials in equation (51) for  $|s_\ell| \ll 1$  giving

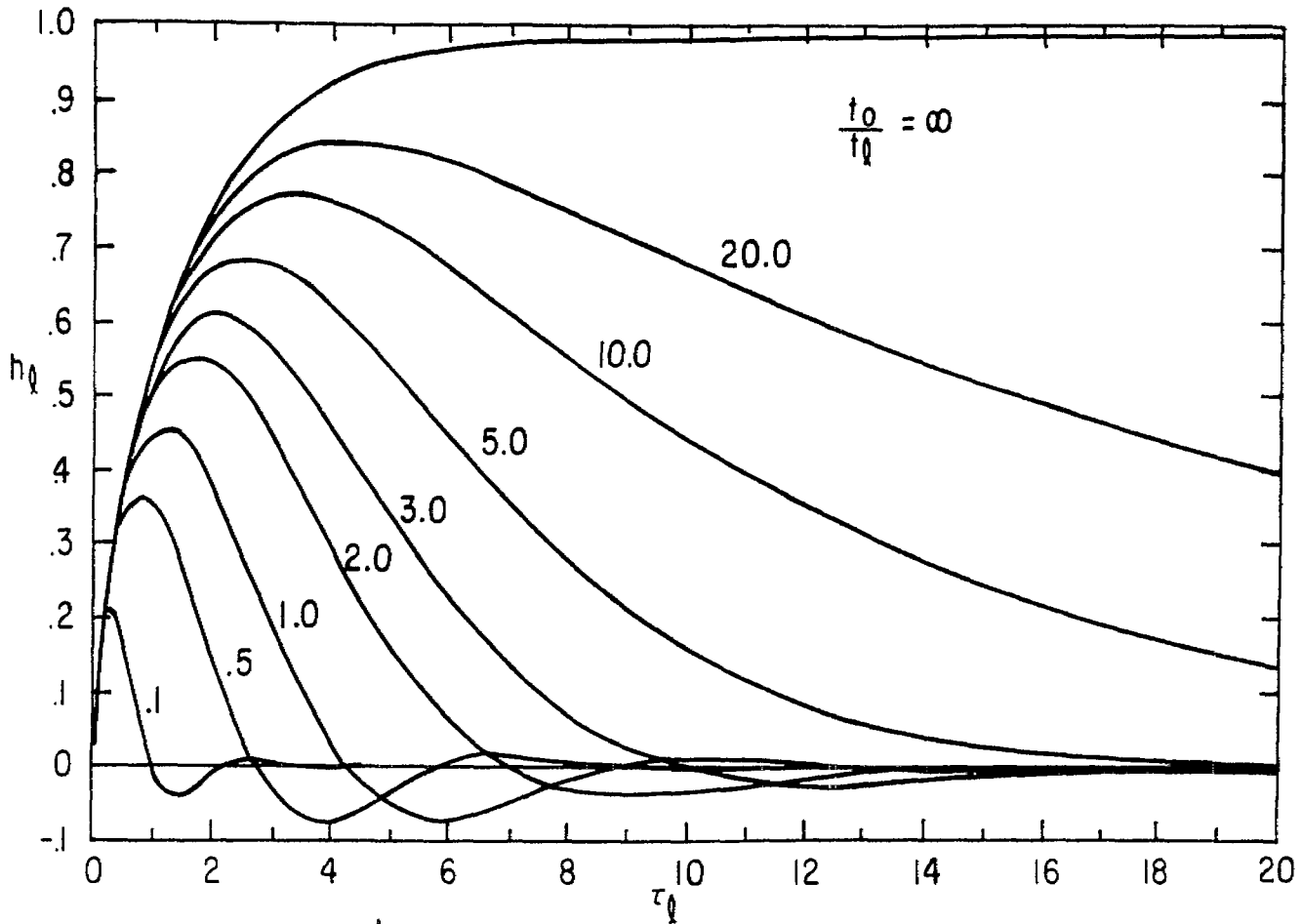
$$\tilde{h}_\ell(s_\ell) \approx (1-z') \left\{ s_\ell + \frac{t_\ell}{t_o} \left[ 1 + \frac{t_a}{t_o} \right]^{-1} \right\}^{-1} \quad (57)$$

In the time domain for  $\tau_\ell \gg 1$  we then have

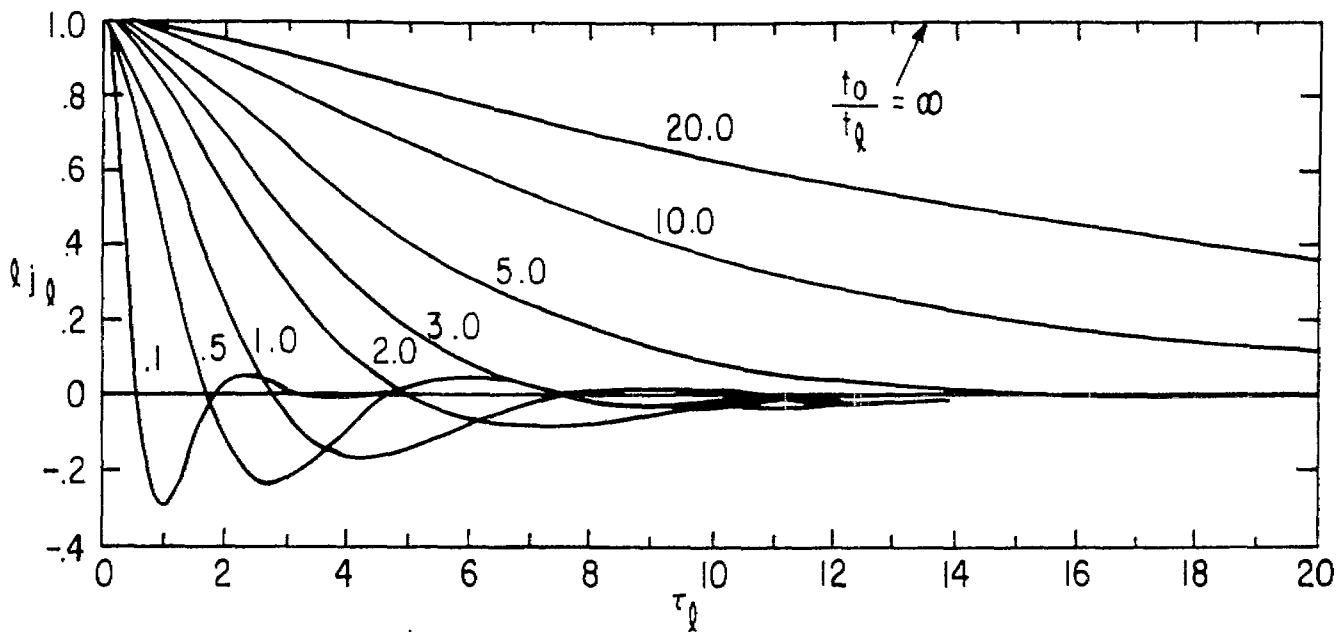
$$h_\ell(\tau_\ell) \approx (1-z) e^{-\tau_\ell \frac{t_\ell}{t_0}} \left[ 1 + \frac{t_a}{t_0} \right]^{-1} = (1-z) e^{-\frac{t}{t_0+t_a}} \quad (58)$$

The time constant for the decay is just  $t_0+t_a$  which is also  $(R_0+R_a)C_G$ , or a simple resistive-capacitive decay. In Figure 12 the maximum value of the magnetic field pulse and the time of this maximum are plotted versus  $t_a/t_\ell$  for 4 values of  $t_0/t_\ell$ . Finally Figure 13 is for the limiting case of large  $C_G$  or equivalently for  $t_0/t_\ell \gg 1$ , in which case we use  $R_a/R_0$  as a parameter for the curves. Note that as  $R_a/R_0$  is increased the rise time of the magnetic field pulse is decreased; but if  $R_0$  and  $V_G$  are fixed then  $I_0$ , the pulse amplitude, is also decreased.

Now go on to include  $z > 0$ . Figures 14 through 17 consider the magnetic field pulse shape. Each figure is for a separate value of  $t_0/t_\ell$ ; each graph in a figure is for a separate  $t_a/t_\ell$ ; each curve on a graph is for a separate  $z$ . This is repeated for the current density in Figures 18 through 21. The maximum of the magnetic field pulse and the time of the maximum are plotted versus  $z'$  in Figures 22 and 23 respectively. Each graph is for a particular  $t_0/t_\ell$ . Finally Figures 24 and 25 give the magnetic field and current density pulse shapes respectively for the limiting case of  $t_0/t_\ell \gg 1$ . Each graph is for a particular  $R_a/R_0$ ; each curve is for a particular  $z'$ .

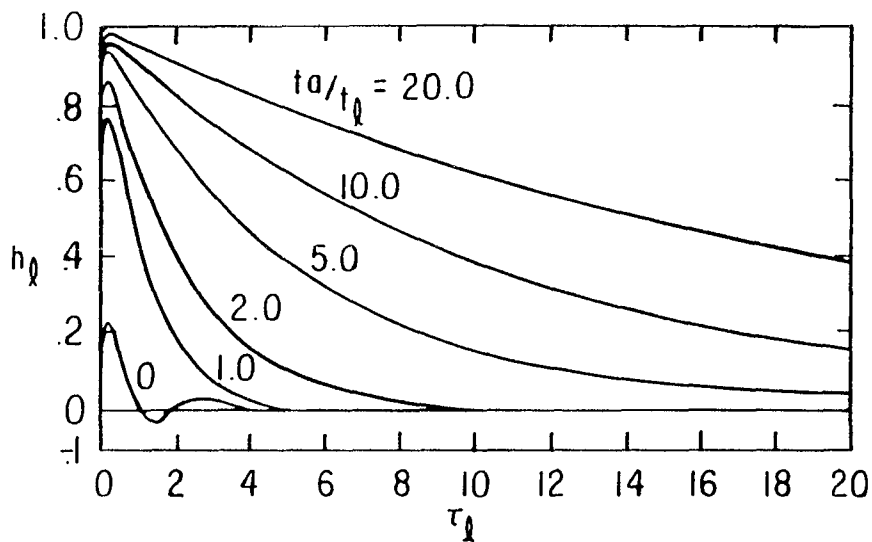


A.  $h_l$  vs  $\tau_l$  WITH  $t_0/t_l$  AS A PARAMETER

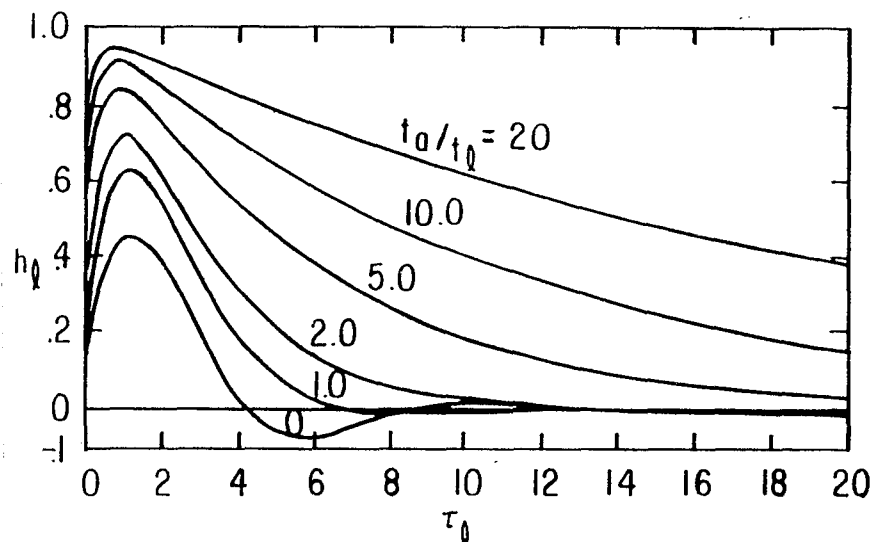


B.  $l_{j_l}$  vs  $\tau_l$  WITH  $t_0/t_l$  AS A PARAMETER

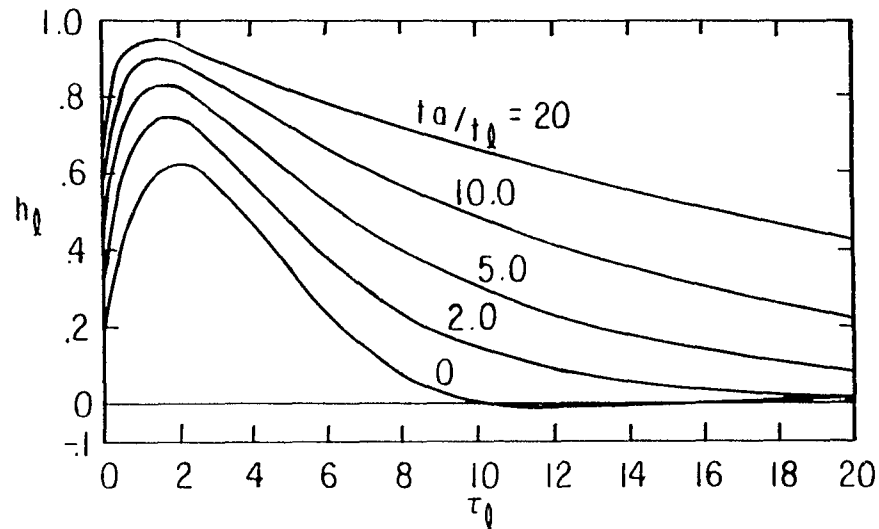
FIGURE 9. PULSE SHAPES AT GROUND SURFACE FOR FINITE LENGTH TRANSMISSION LINE:  $z' = 0, t_0/t_l = 0$



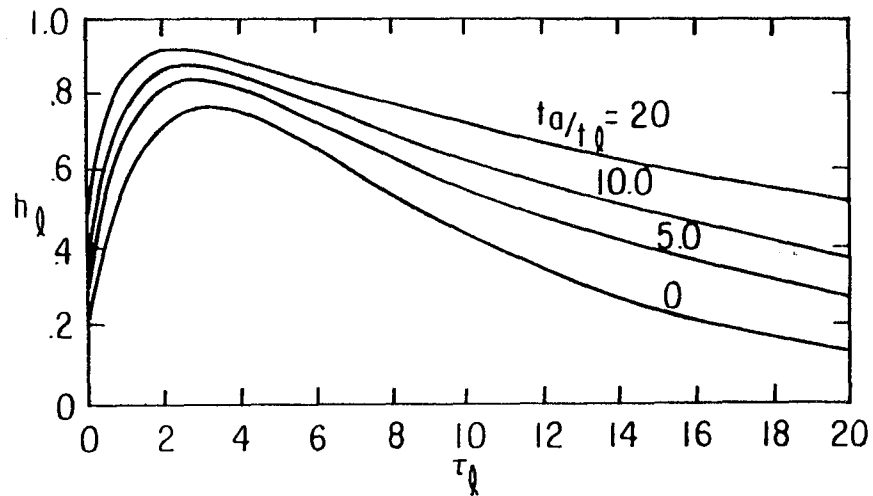
A.  $h_l$  vs  $\tau_l$  WITH  $t_a/t_l$  AS A PARAMETER:  $t_0/t_l = .1$



B.  $h_l$  vs  $\tau_l$  WITH  $t_a/t_l$  AS A PARAMETER:  $t_0/t_l = 1.0$

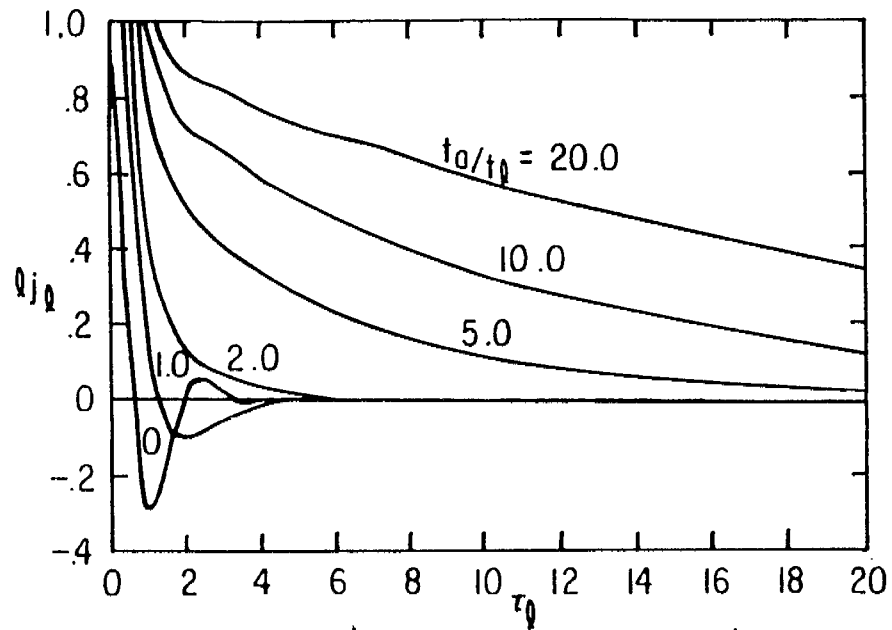


C.  $h_l$  vs  $\tau_l$  WITH  $t_a/t_l$  AS A PARAMETER:  $t_0/t_l = 3$

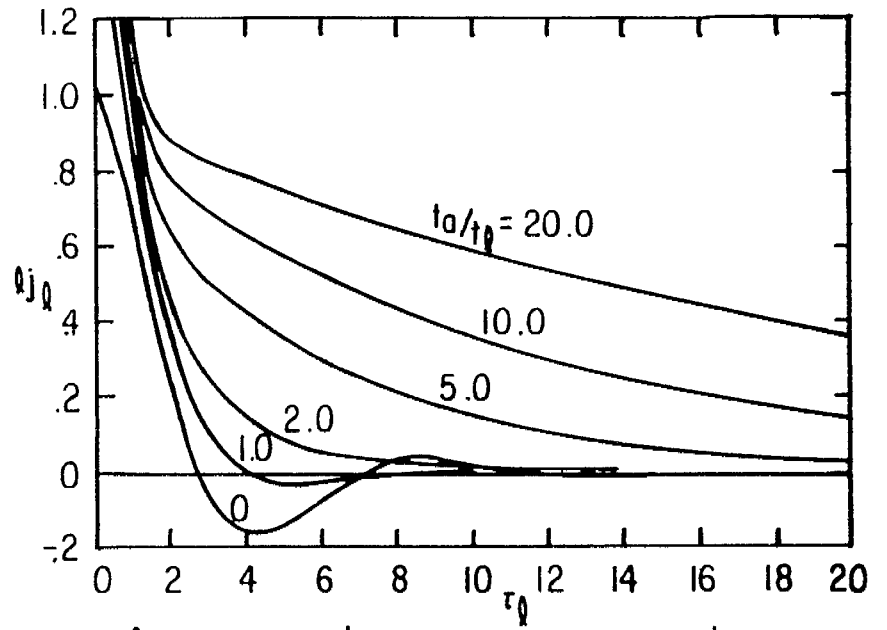


D.  $h_l$  vs  $\tau_l$  WITH  $t_a/t_l$  AS A PARAMETER:  $t_0/t_l = 10$

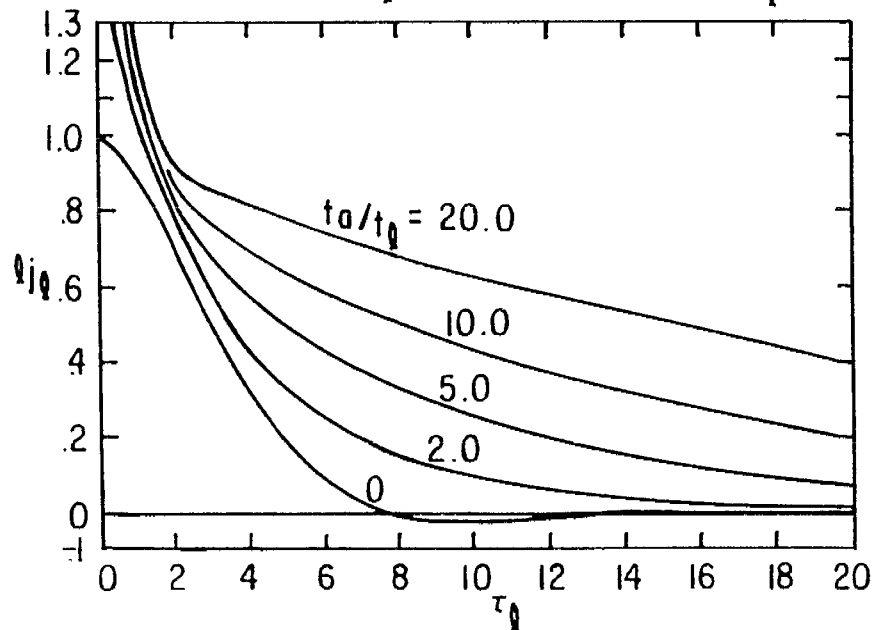
FIGURE 10. CURRENT OR MAGNETIC FIELD PULSE SHAPE FOR FINITE LENGTH TRANSMISSION LINE:  $z' = 0$



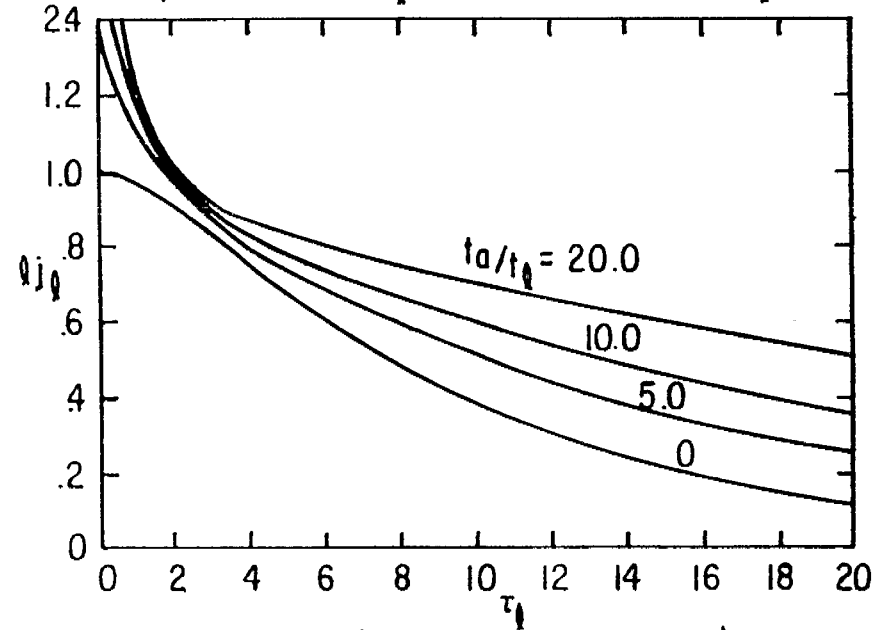
A.  $q_{j0}$  vs  $\tau_0$  WITH  $t_0/t_0$  AS A PARAMETER:  $t_0/t_0 = .1$



B.  $q_{j0}$  vs  $\tau_0$  WITH  $t_0/t_0$  AS A PARAMETER:  $t_0/t_0 = 1.0$

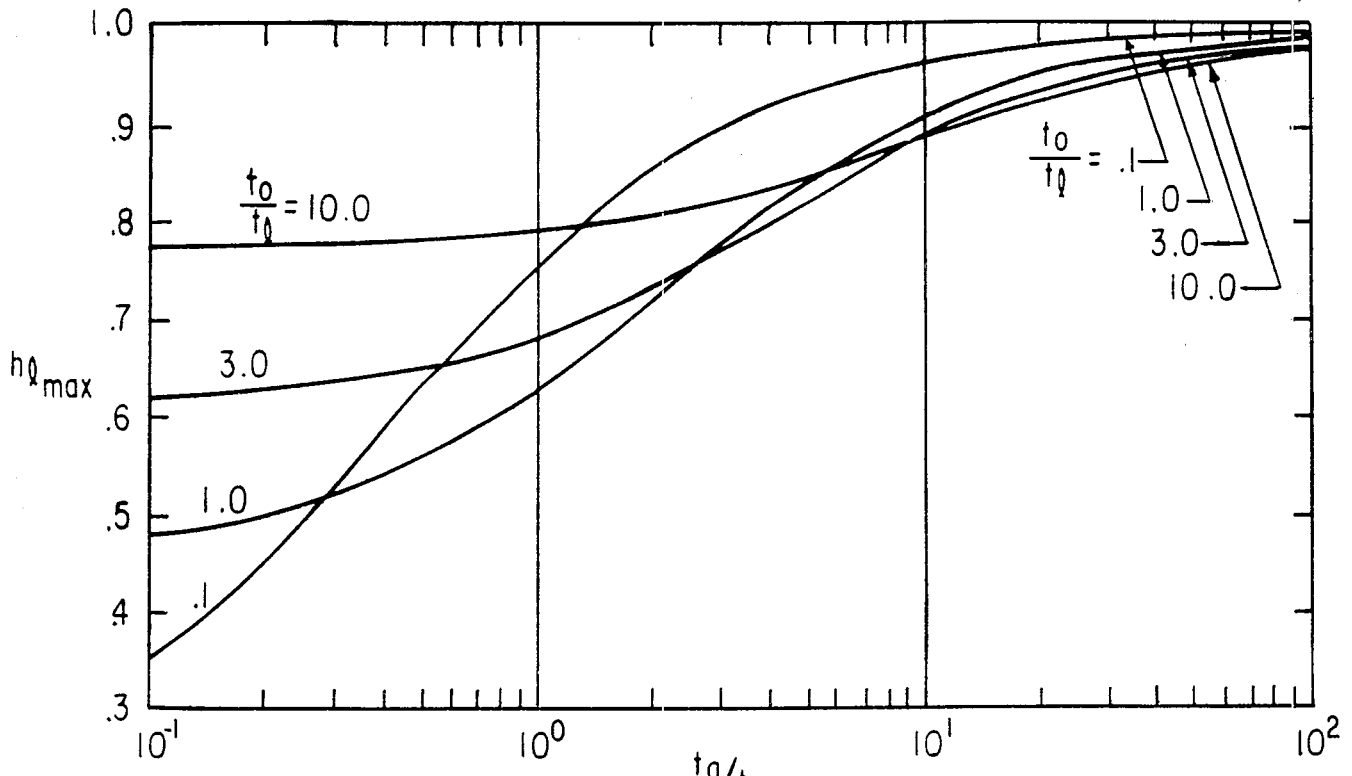


C.  $q_{j0}$  vs  $\tau_0$  WITH  $t_0/t_0$  AS A PARAMETER:  $t_0/t_0 = 3$

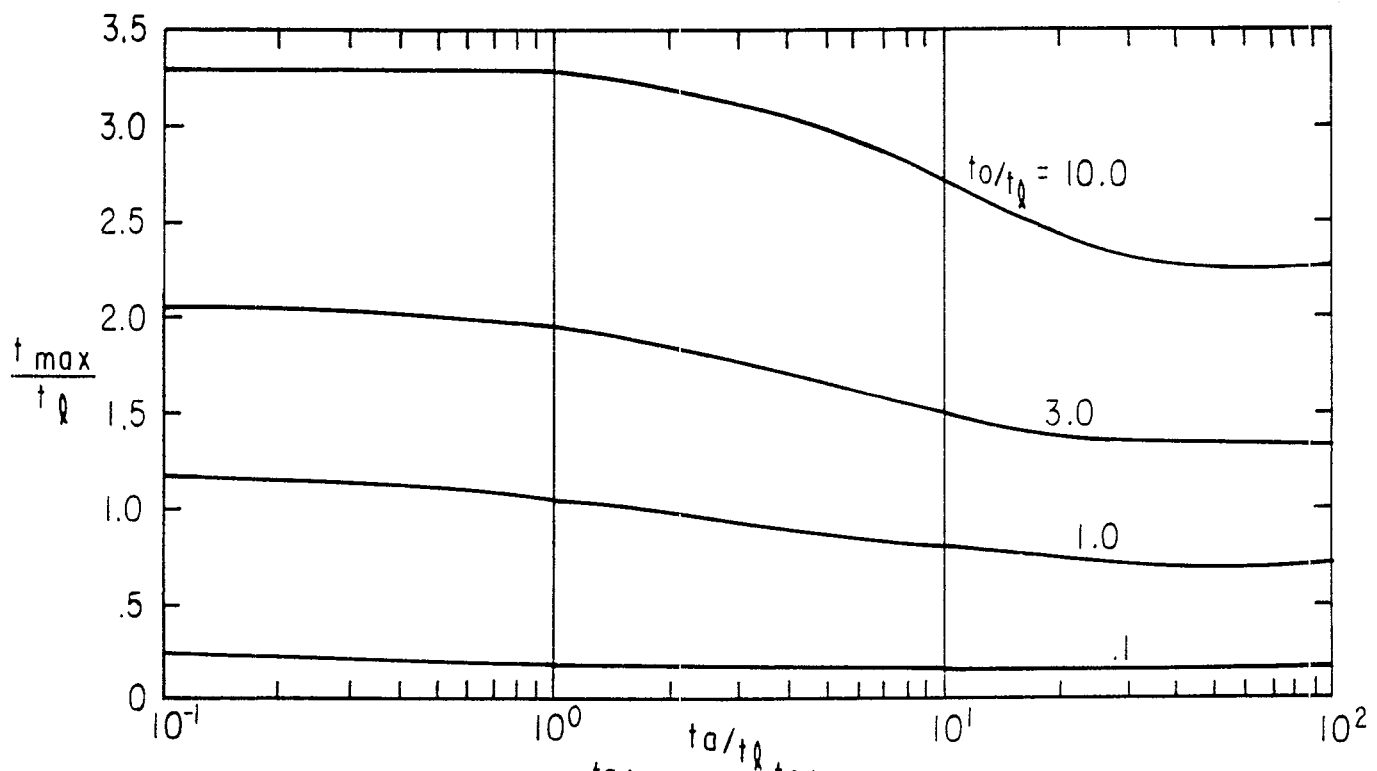


D.  $q_{j0}$  vs  $\tau_0$  WITH  $t_0/t_0$  AS A PARAMETER:  $t_0/t_0 = 10$

FIGURE II. VOLTAGE OR CURRENT DENSITY PULSE SHAPE FOR FINITE LENGTH TRANSMISSION LINE:  $z' = 0$

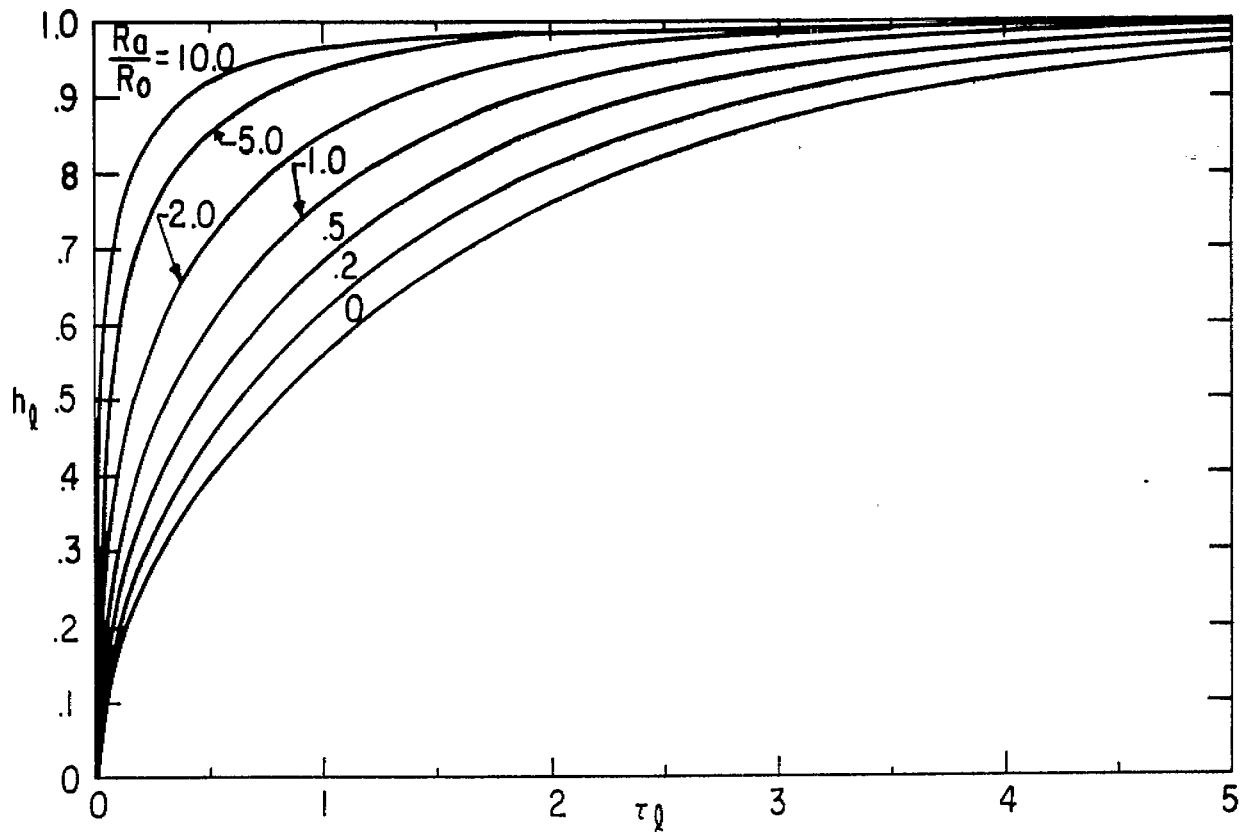


A. VALUE OF MAXIMUM vs  $t_a/t_q$  WITH  $t_o/t_q$  AS A PARAMETER

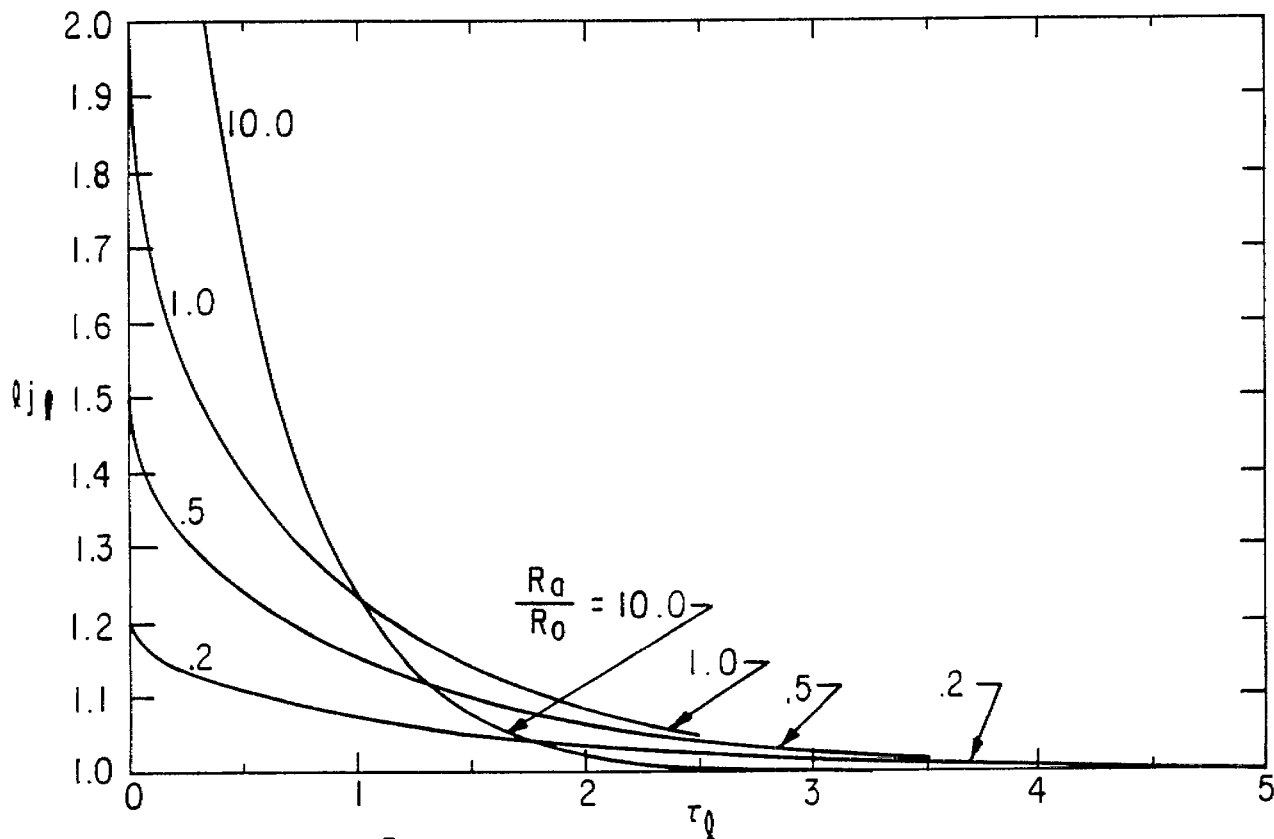


B. TIME OF MAXIMUM vs.  $t_a/t_q$  WITH  $t_o/t_q$  AS A PARAMETER

FIGURE 12. PARAMETERS OF CURRENT OR MAGNETIC FIELD PULSE SHAPE AT GROUND SURFACE FOR FINITE LENGTH TRANSMISSION LINE:  $z' = 0$

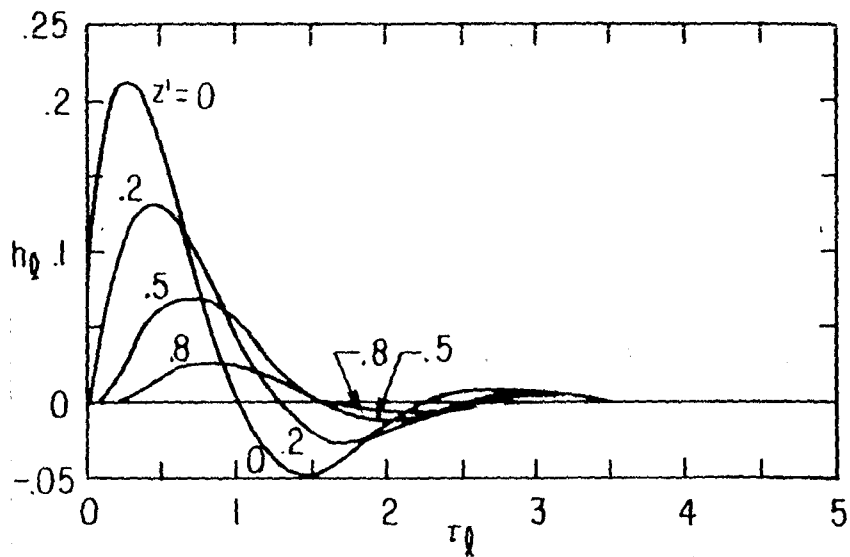


A.  $h_q$  vs  $\tau_q$  WITH  $R_a/R_0$  AS A PARAMETER

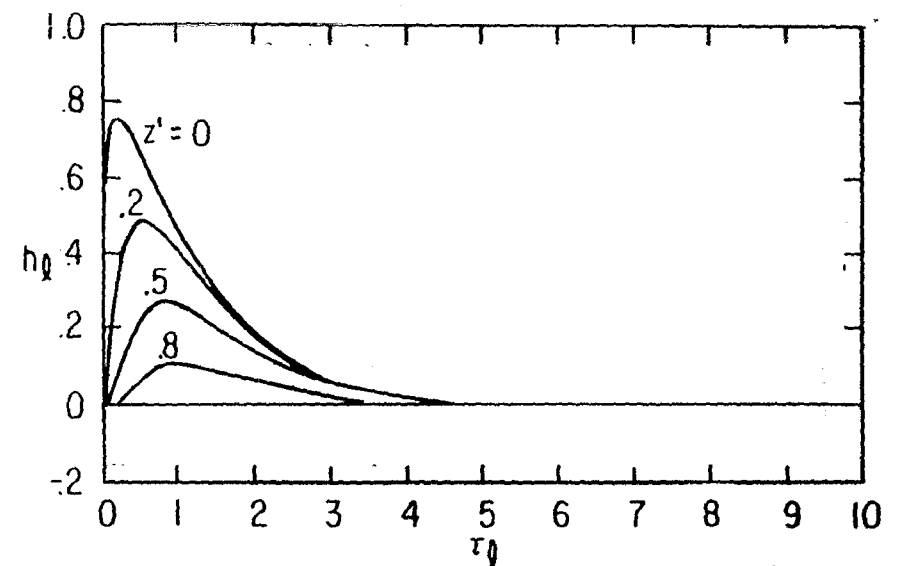


B.  $q_j$  vs  $\tau_q$  WITH  $R_a/R_0$  AS A PARAMETER

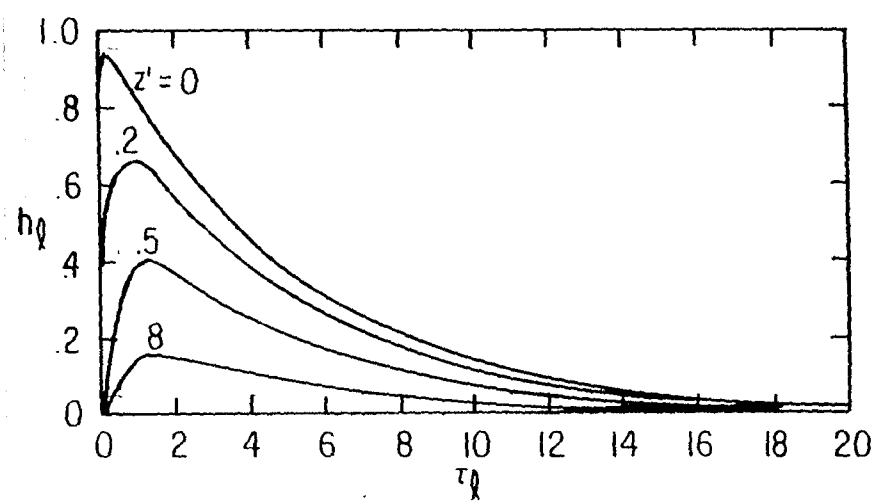
FIGURE 13. PULSE SHAPES AT GROUND SURFACE FOR FINITE LENGTH TRANSMISSION LINE AND INFINITE GENERATOR CAPACITANCE:  $z'=0$



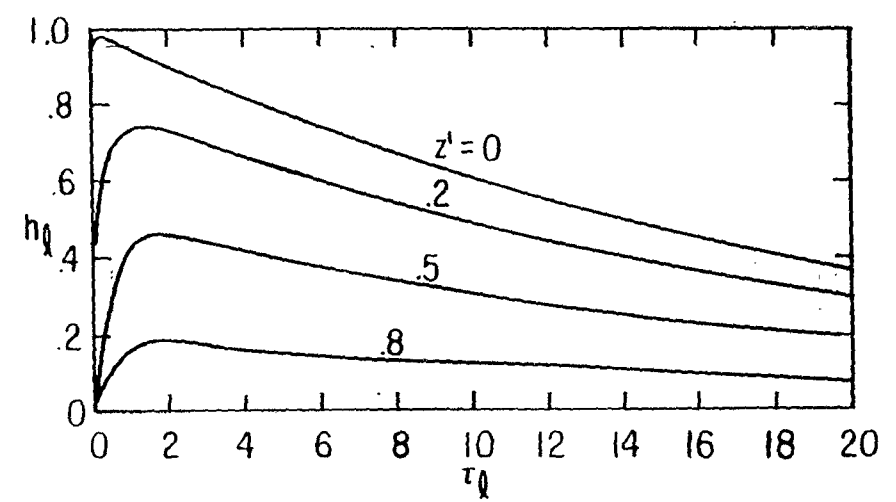
A.  $h_q$  vs  $\tau_q$  WITH  $z'$  AS A PARAMETER:  $t_0/t_q = 0$



B.  $h_q$  vs  $\tau_q$  WITH  $z'$  AS A PARAMETER:  $t_0/t_q = 1$

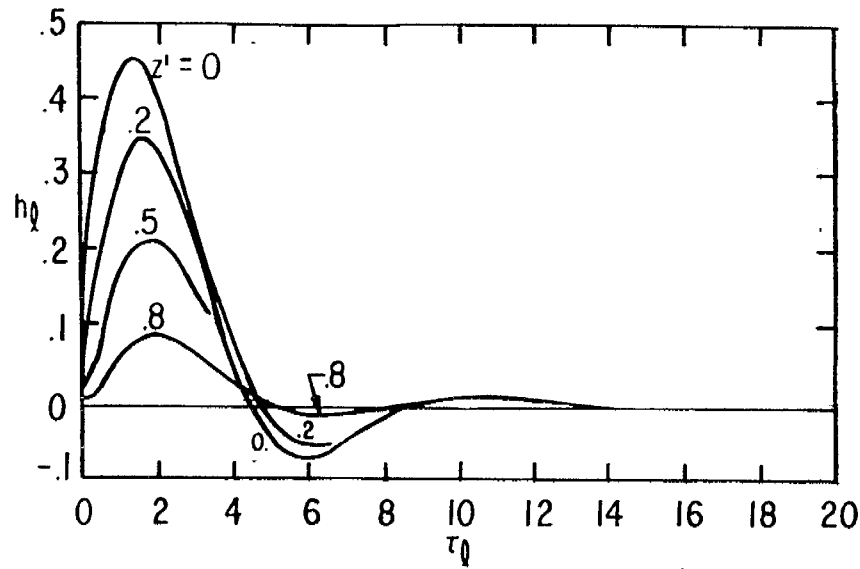


C.  $h_q$  vs  $\tau_q$  WITH  $z'$  AS A PARAMETER:  $t_0/t_q = 5$

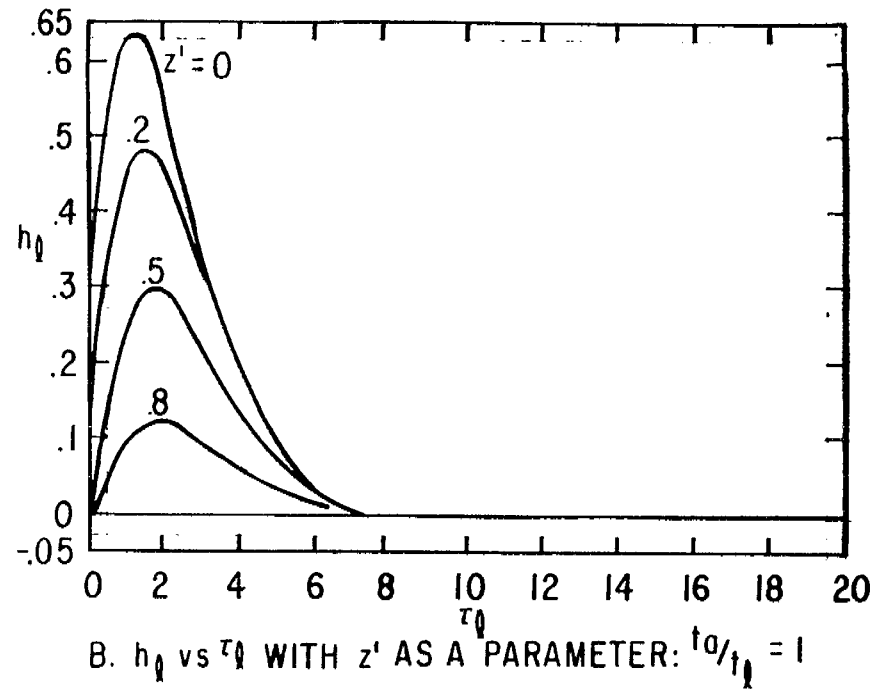


D.  $h_q$  vs  $\tau_q$  WITH  $z'$  AS A PARAMETER:  $t_0/t_q = 20$

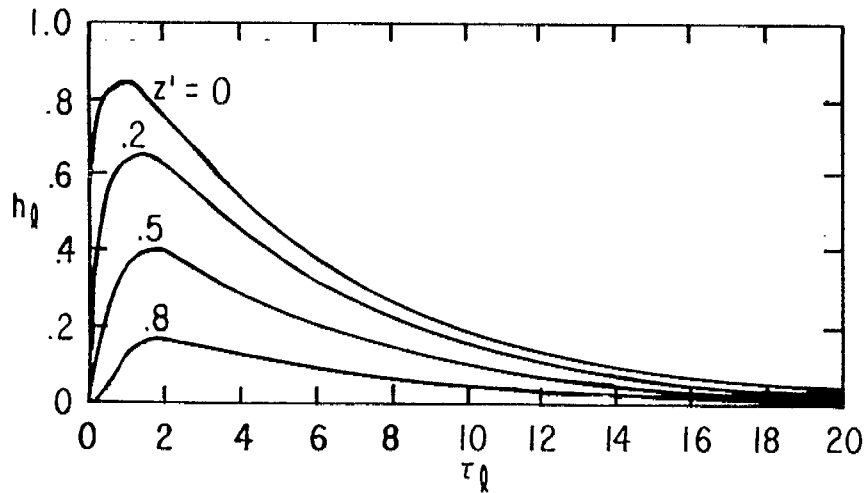
FIGURE 14. CURRENT OR MAGNETIC FIELD PULSE SHAPE FOR FINITE LENGTH TRANSMISSION LINE:  $t_0/t_q = .1$



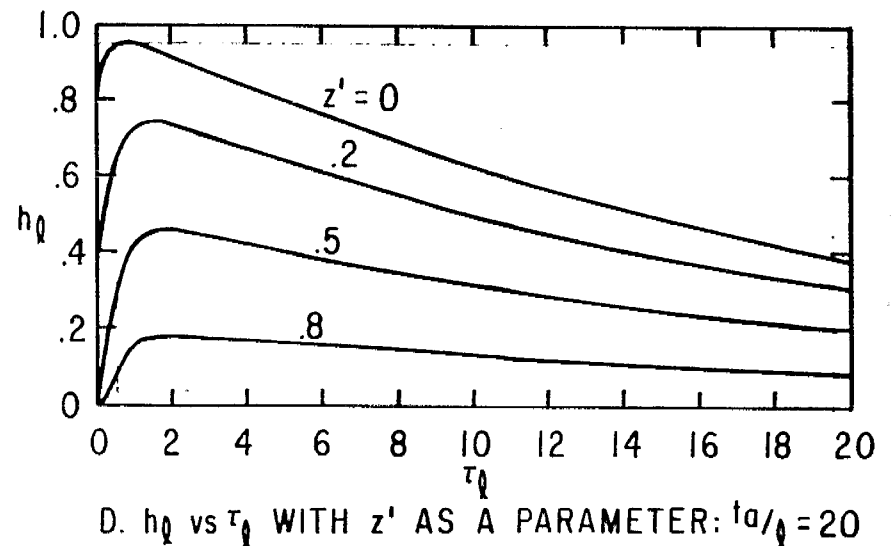
A.  $h_q$  vs  $\tau_q$  WITH  $z'$  AS A PARAMETER:  $t_0/t_q = 0$



B.  $h_q$  vs  $\tau_q$  WITH  $z'$  AS A PARAMETER:  $t_0/t_q = 1$

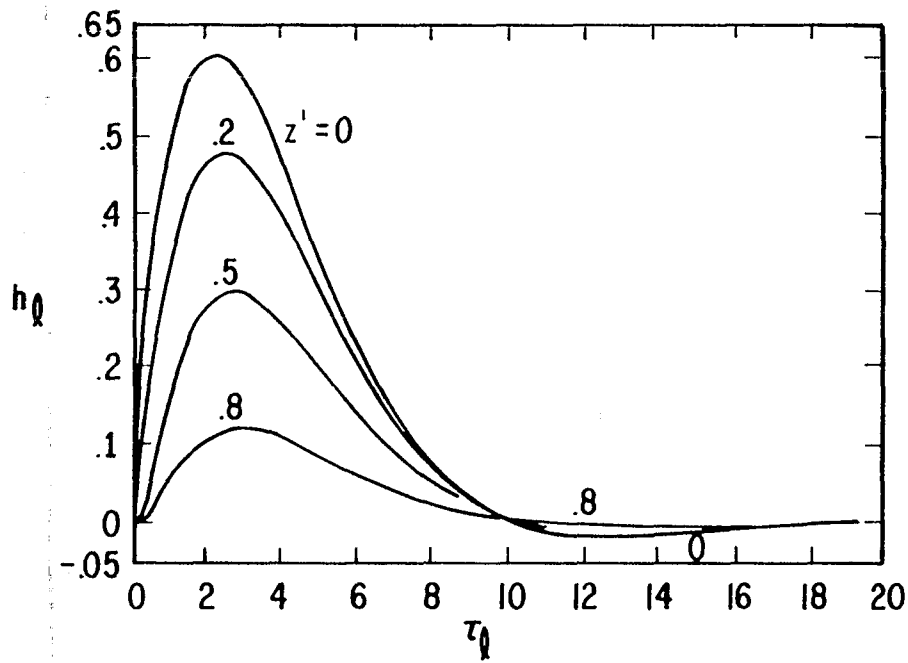


C.  $h_q$  vs  $\tau_q$  WITH  $z'$  AS A PARAMETER:  $t_0/t_q = 5$

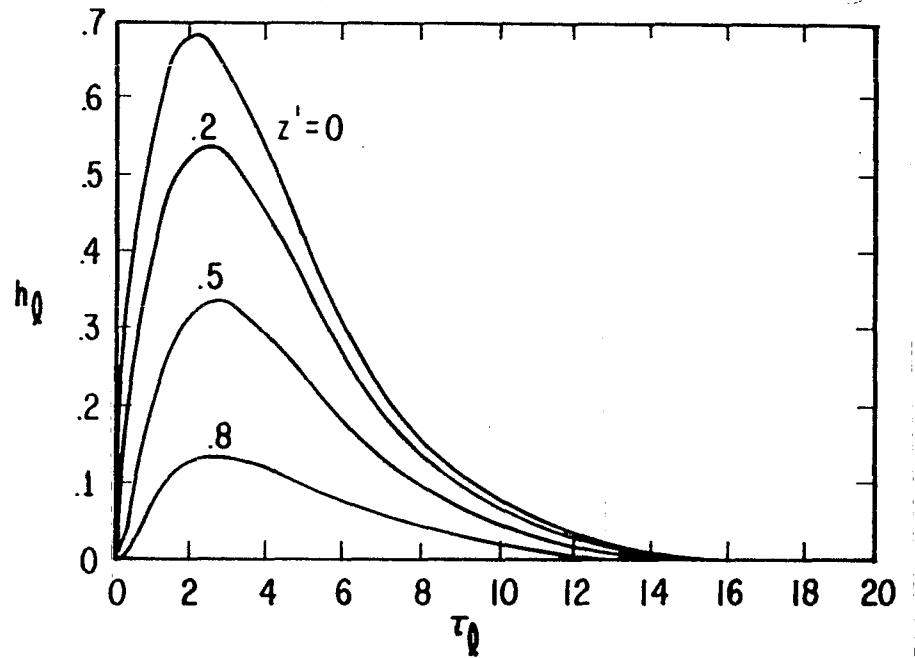


D.  $h_q$  vs  $\tau_q$  WITH  $z'$  AS A PARAMETER:  $t_0/t_q = 20$

FIGURE 15. CURRENT OR MAGNETIC FIELD PULSE SHAPE FOR FINITE LENGTH TRANSMISSION LINE:  $t_0/t_q = 1$

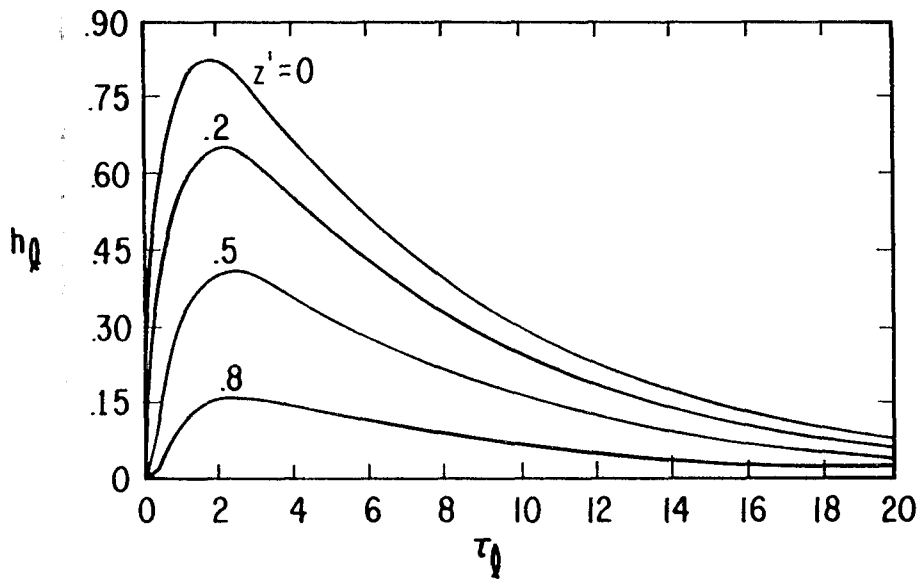


A.  $h_0$  vs  $\tau_0$  WITH  $z'$  AS A PARAMETER:  $t_0/t_0 = 0$

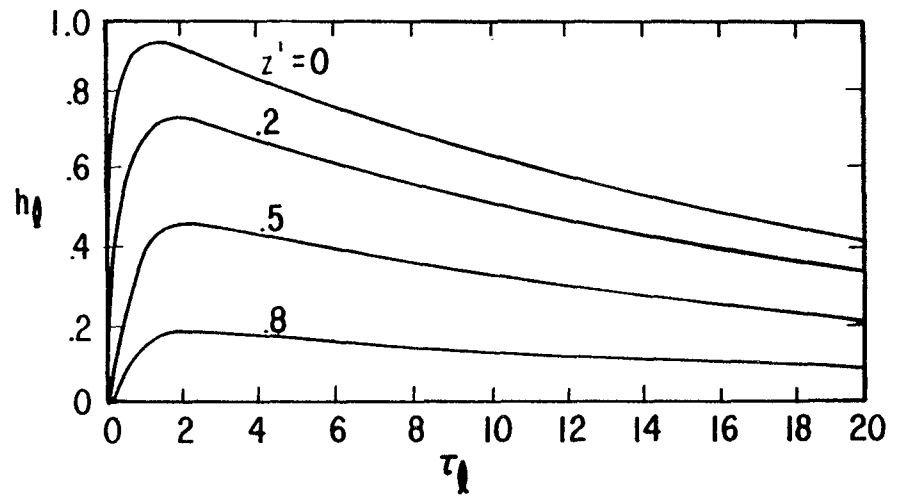


B.  $h_0$  vs  $\tau_0$  WITH  $z'$  AS A PARAMETER:  $t_0/t_0 = 1$

31

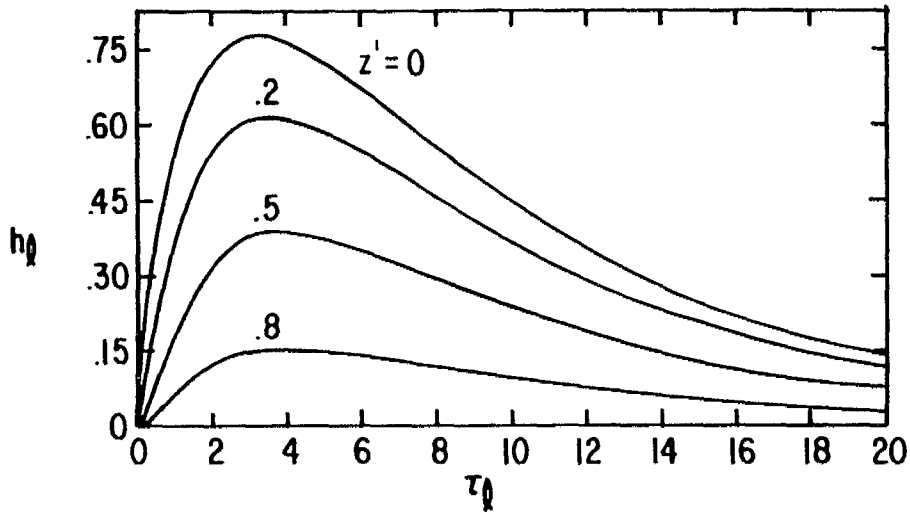


C.  $h_0$  vs  $\tau_0$  WITH  $z'$  AS A PARAMETER:  $t_0/t_0 = 5$

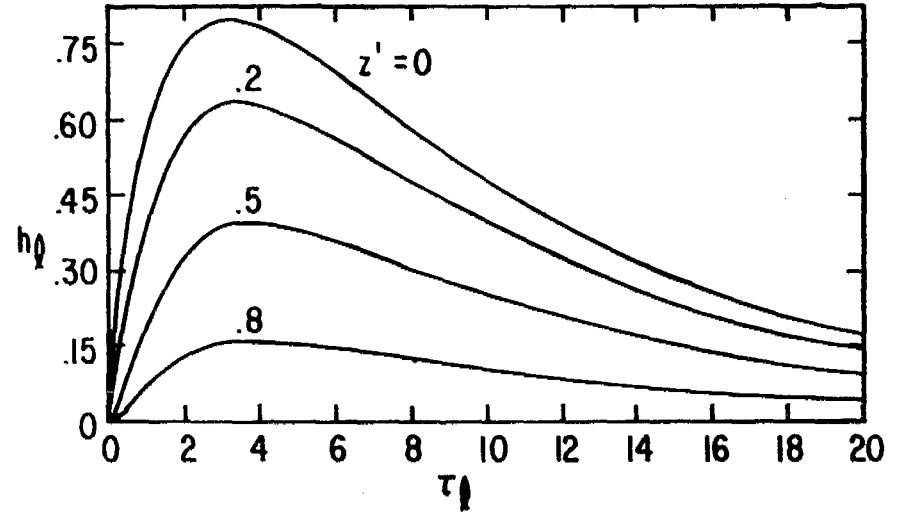


D.  $h_0$  vs  $\tau_0$  WITH  $z'$  AS A PARAMETER:  $t_0/t_0 = 20$

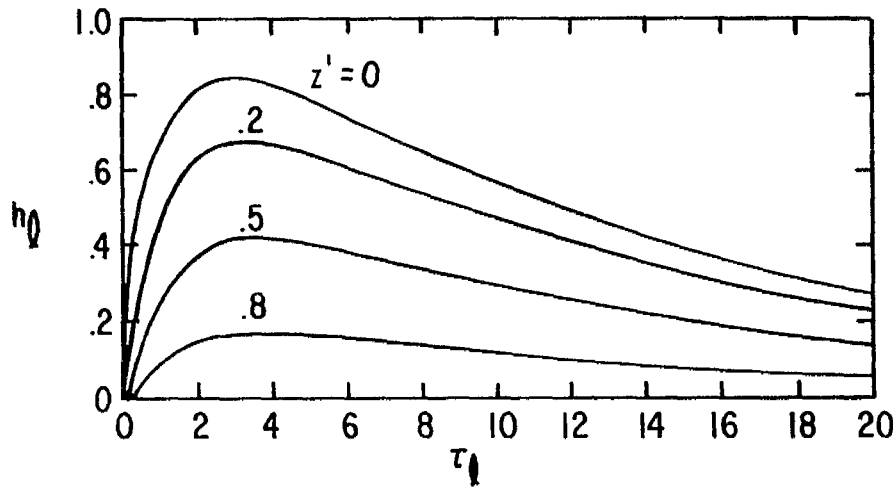
FIGURE 16. CURRENT OR MAGNETIC FIELD PULSE SHAPE FOR FINITE LENGTH TRANSMISSION LINE:  $t_0/t_0 = 3$



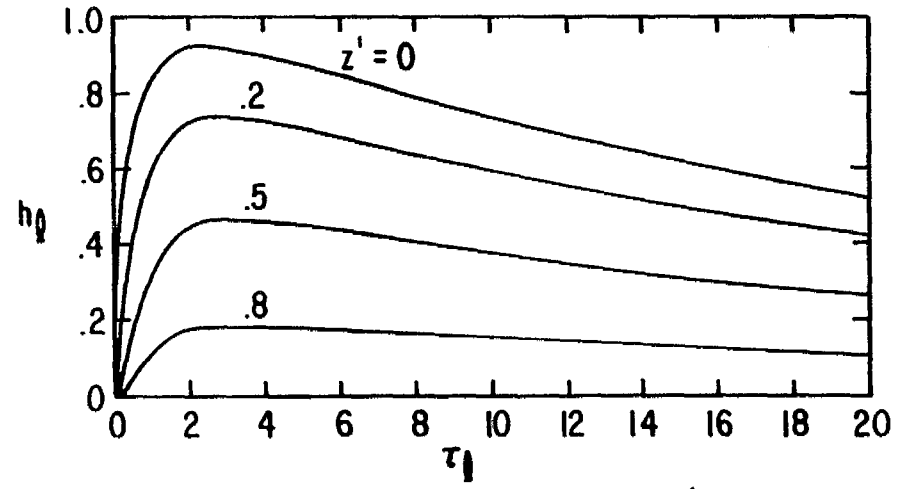
A.  $h_0$  vs  $\tau_0$  WITH  $z'$  AS A PARAMETER:  $t_0/t_1 = 0$



B.  $h_0$  vs  $\tau_0$  WITH  $z'$  AS A PARAMETER:  $t_0/t_1 = 1$

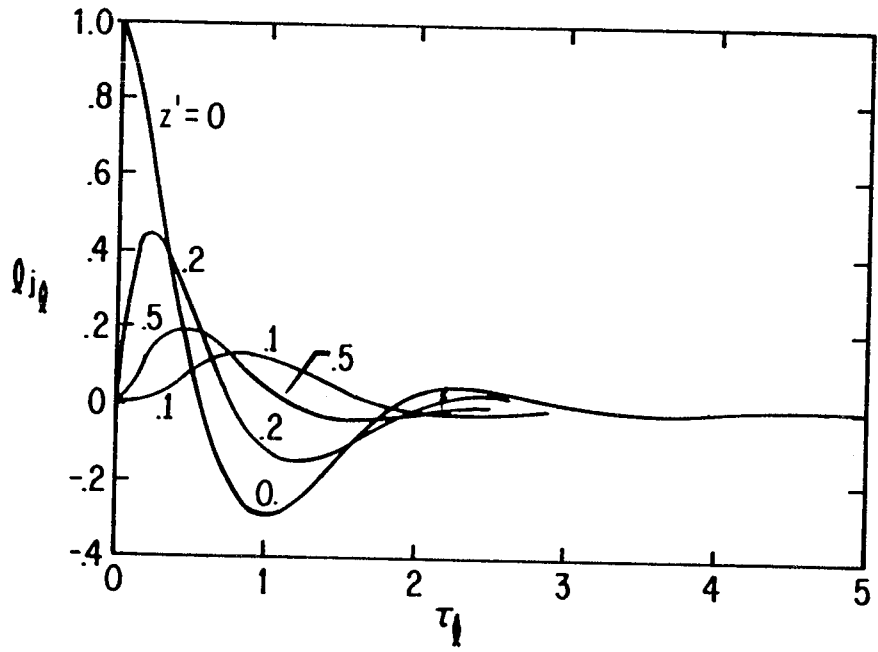


C.  $h_0$  vs  $\tau_0$  WITH  $z'$  AS A PARAMETER:  $t_0/t_1 = 5$

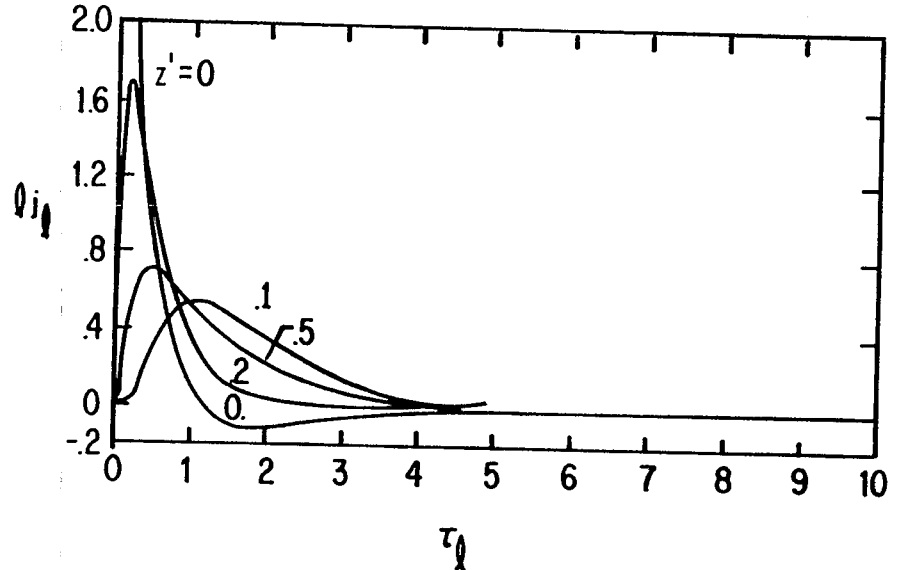


D.  $h_0$  vs  $\tau_0$  WITH  $z'$  AS A PARAMETER:  $t_0/t_1 = 20$

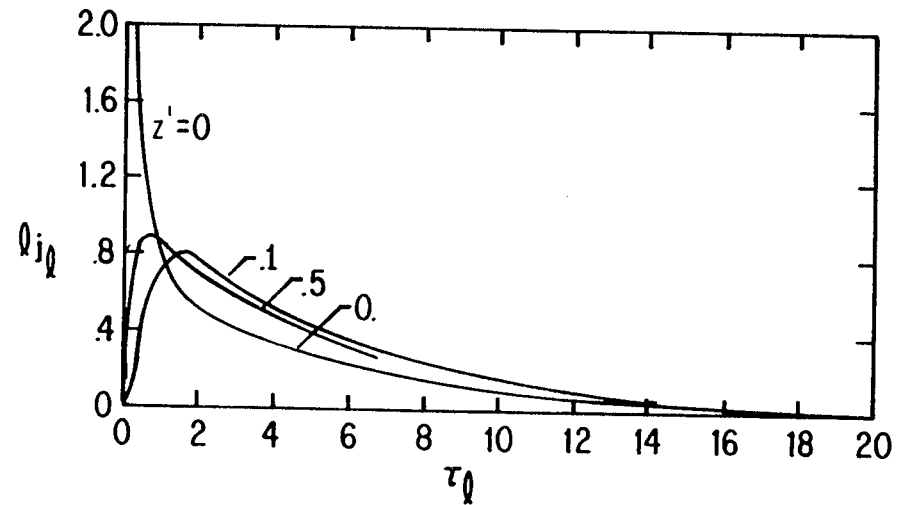
FIGURE 17. CURRENT OR MAGNETIC FIELD PULSE SHAPE FOR FINITE LENGTH TRANSMISSION LINE:  $t_0/t_1 = 10$



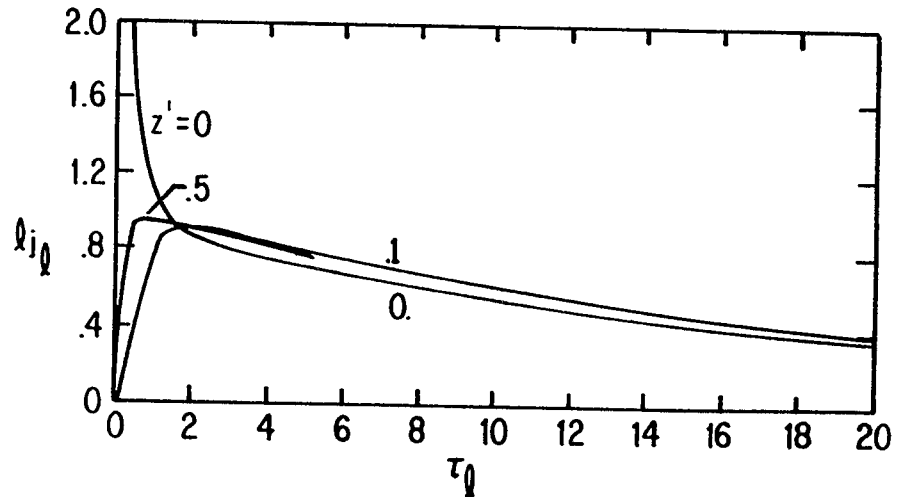
A.  $Q_{j\ell}$  vs  $\tau_{\ell}$  WITH  $z'$  AS A PARAMETER:  $t_0/t_{\ell} = 0$



B.  $Q_{j\ell}$  vs  $\tau_{\ell}$  WITH  $z'$  AS A PARAMETER:  $t_0/t_{\ell} = 1$

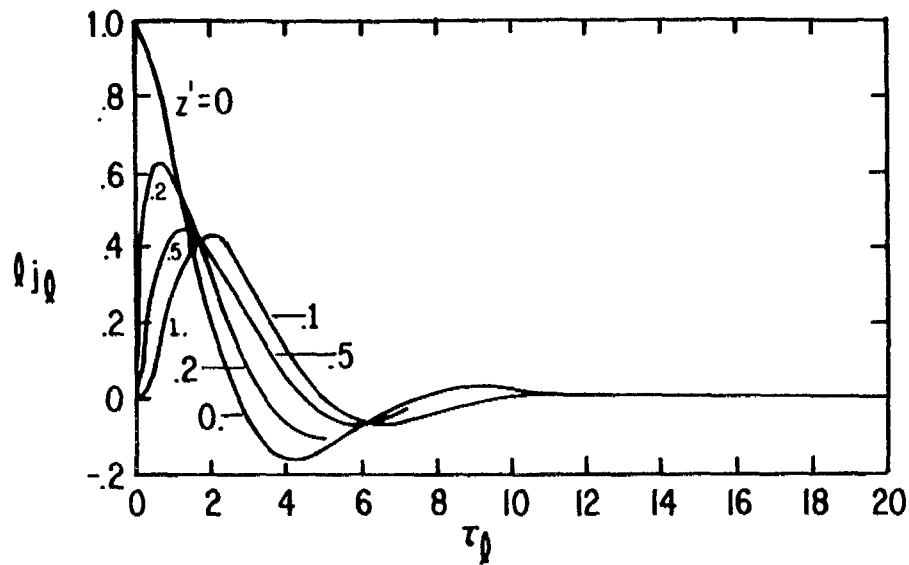


C.  $Q_{j\ell}$  vs  $\tau_{\ell}$  WITH  $z'$  AS A PARAMETER:  $t_0/t_{\ell} = 5$

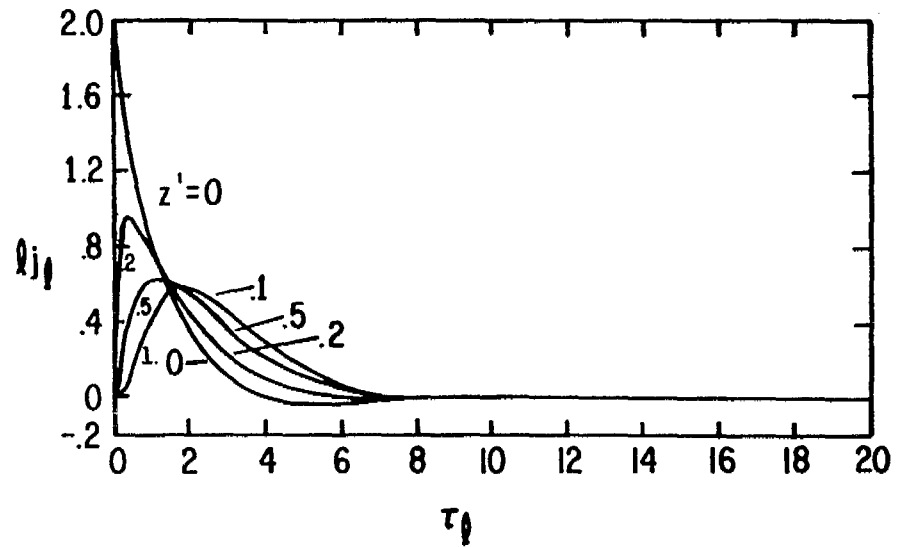


D.  $Q_{j\ell}$  vs  $\tau_{\ell}$  WITH  $z'$  AS A PARAMETER:  $t_0/t_{\ell} = 20$

FIGURE 18. VOLTAGE OR CURRENT DENSITY PULSE SHAPE FOR FINITE LENGTH TRANSMISSION LINE :  $t_0/t_{\ell} = .1$

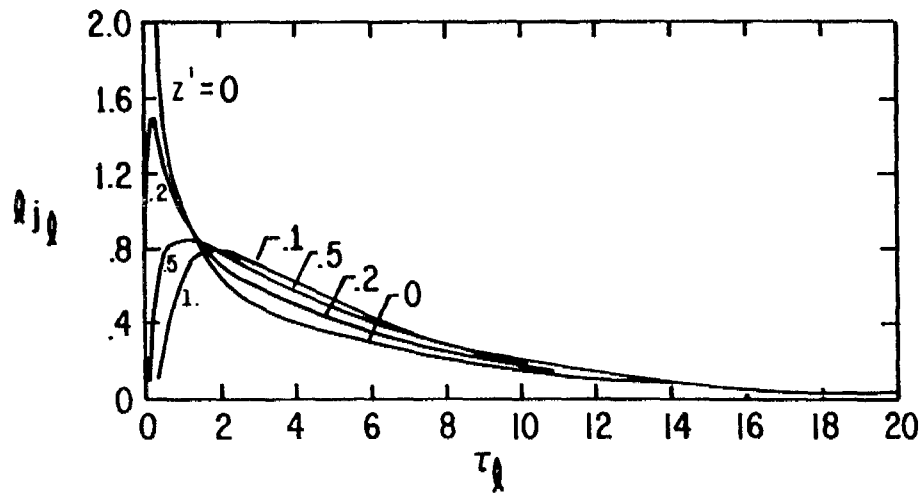


A.  $Q_{jl}$  vs  $\tau_l$  WITH  $z'$  AS A PARAMETER:  $t_0/t_l = 0$

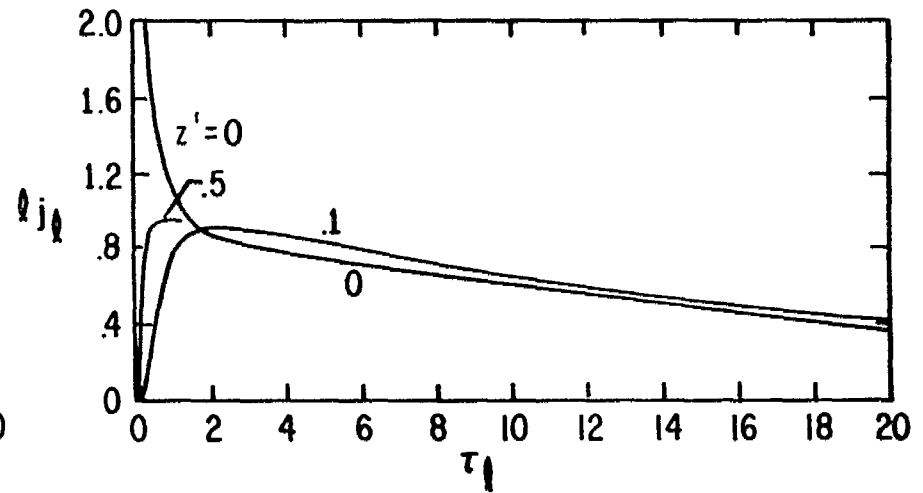


B.  $Q_{jl}$  vs  $\tau_l$  WITH  $z'$  AS A PARAMETER:  $t_0/t_l = 1$

34

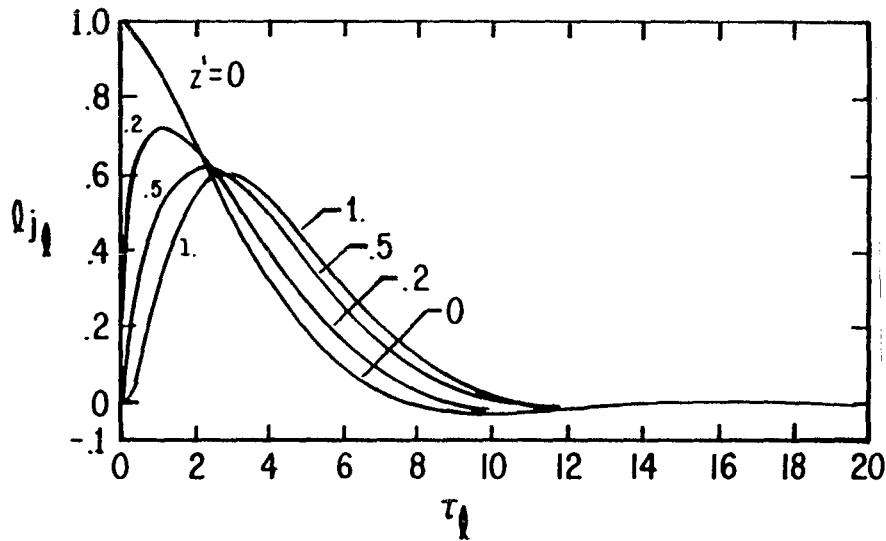


C.  $Q_{jl}$  vs  $\tau_l$  WITH  $z'$  AS A PARAMETER:  $t_0/t_l = 5$

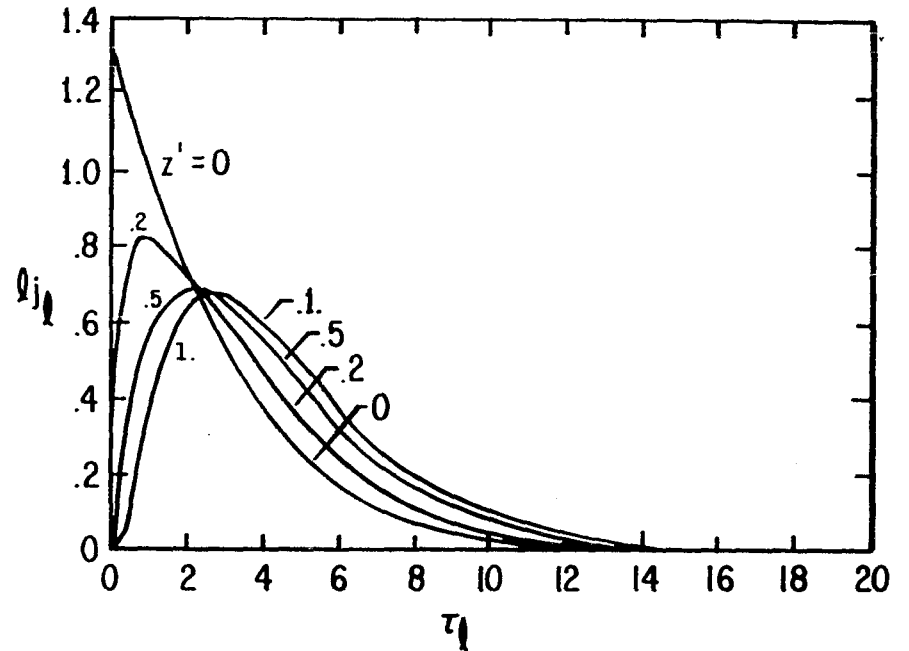


D.  $Q_{jl}$  vs  $\tau_l$  WITH  $z'$  AS A PARAMETER:  $t_0/t_l = 20$

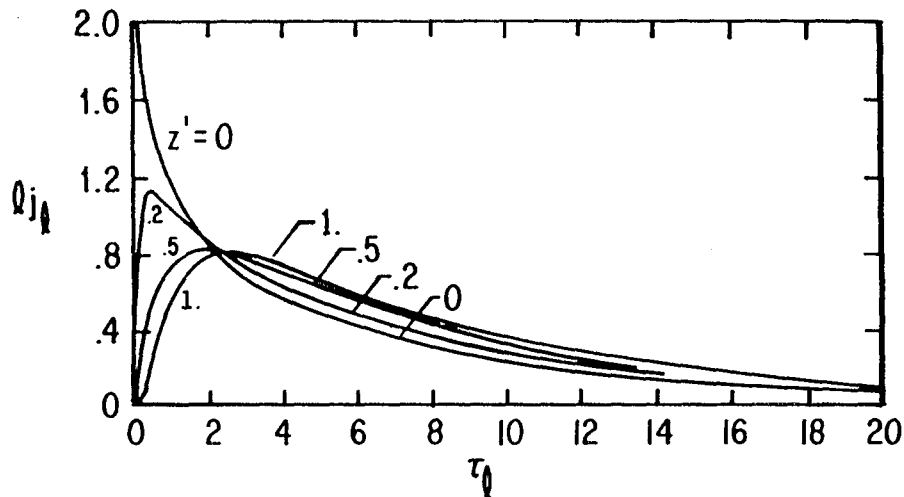
FIGURE 19. VOLTAGE OR CURRENT DENSITY PULSE SHAPE FOR FINITE LENGTH TRANSMISSION LINE:  $t_0/t_l = 1$



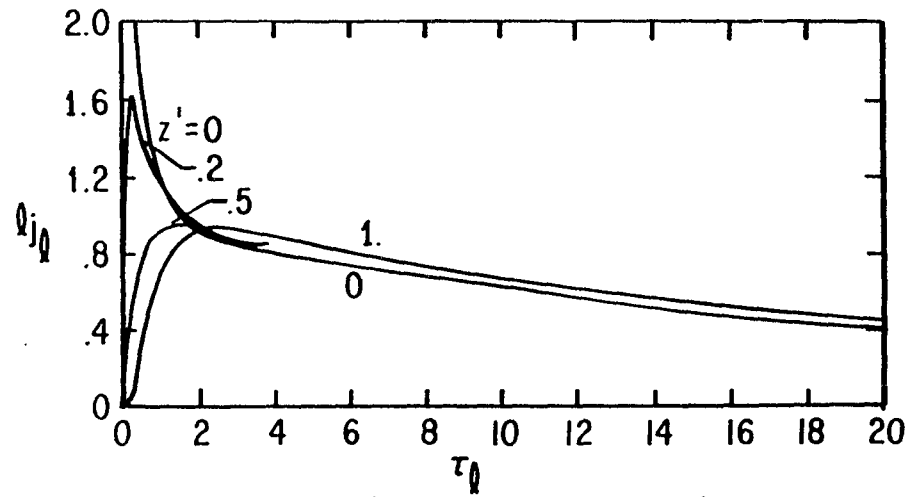
A.  $Q_{jQ}$  vs  $\tau_Q$  WITH  $z'$  AS A PARAMETER:  $t_a/t_Q = 0$



B.  $Q_{jQ}$  vs  $\tau_Q$  WITH  $z'$  AS A PARAMETER:  $t_a/t_Q = 1$

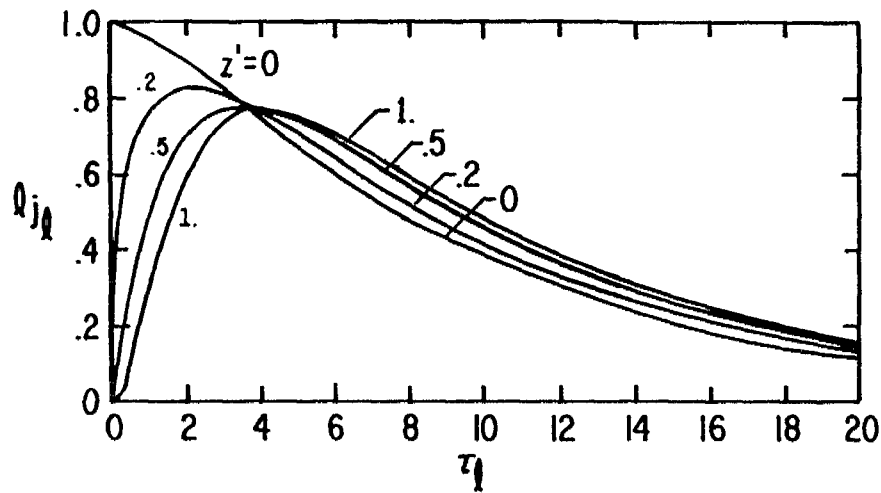


C.  $Q_{jQ}$  vs  $\tau_Q$  WITH  $z'$  AS A PARAMETER:  $t_a/t_Q = 5$

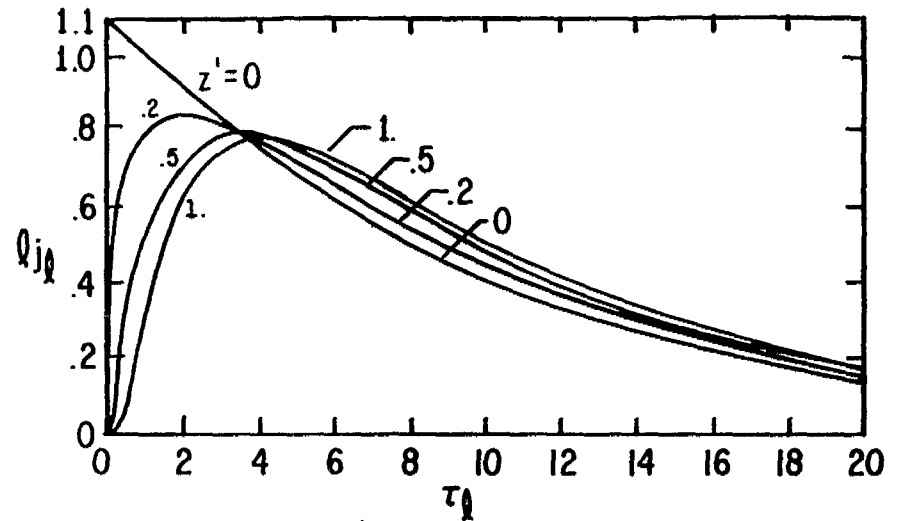


D.  $Q_{jQ}$  vs  $\tau_Q$  WITH  $z'$  AS A PARAMETER:  $t_a/t_Q = 20$

FIGURE 20. VOLTAGE OR CURRENT DENSITY PULSE SHAPE FOR FINITE LENGTH TRANSMISSION LINE :  $t_a/t_Q = 3$

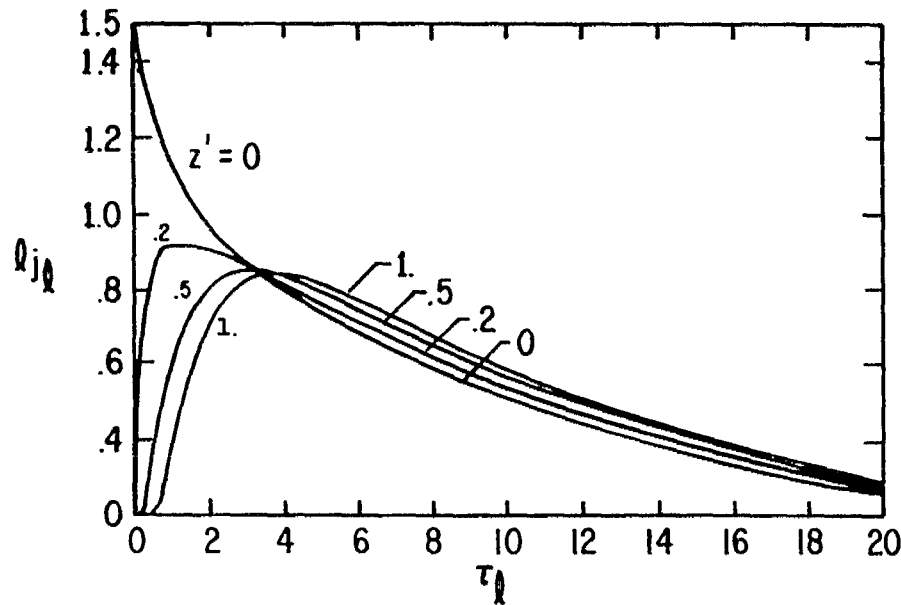


A.  $Q_{j_l}$  vs  $\tau_l$  WITH  $z'$  AS A PARAMETER:  $t_0/t_l = 0$

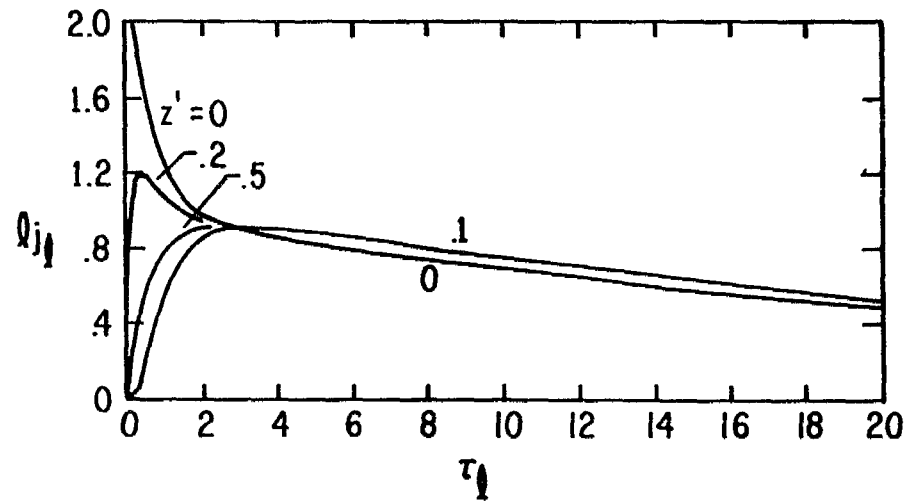


B.  $Q_{j_l}$  vs  $\tau_l$  WITH  $z'$  AS A PARAMETER:  $t_0/t_l = 1$

36

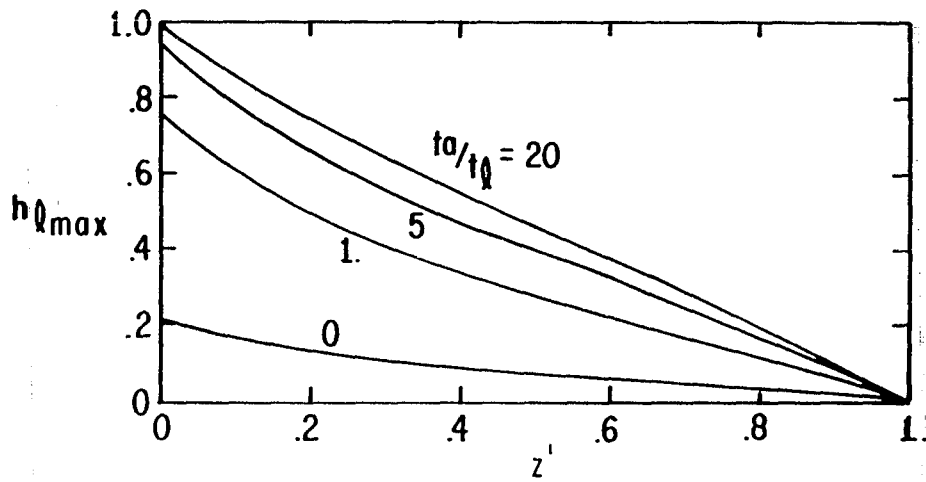


C.  $Q_{j_l}$  vs  $\tau_l$  WITH  $z'$  AS A PARAMETER:  $t_0/t_l = 5$

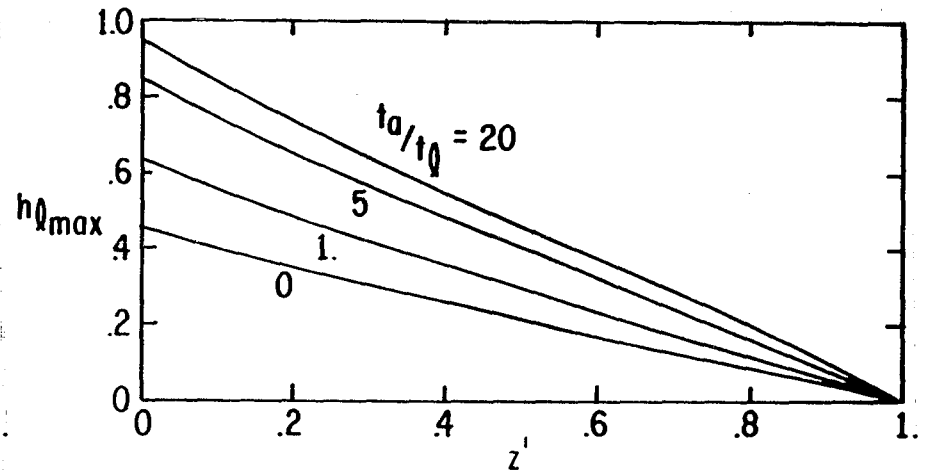


D.  $Q_{j_l}$  vs  $\tau_l$  WITH  $z'$  AS A PARAMETER:  $t_0/t_l = 20$

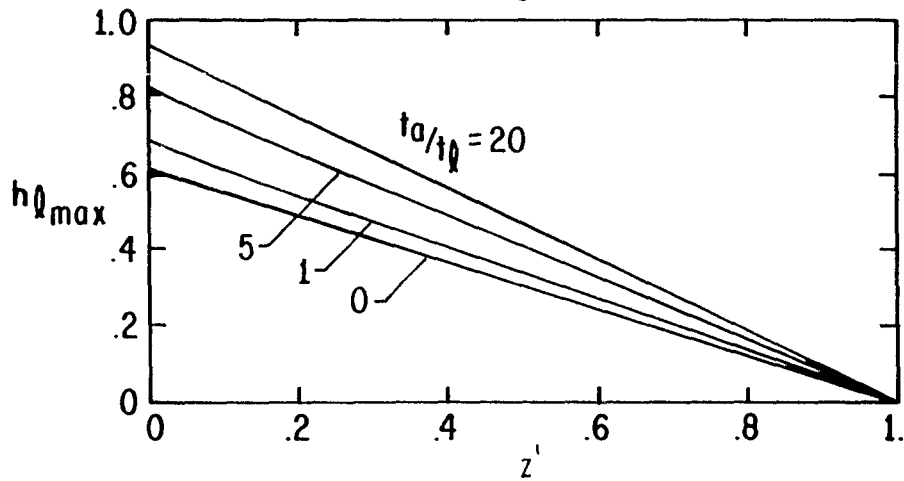
FIGURE 21. VOLTAGE OR CURRENT DENSITY PULSE SHAPE FOR FINITE LENGTH TRANSMISSION LINE:  $t_0/t_l = 10$



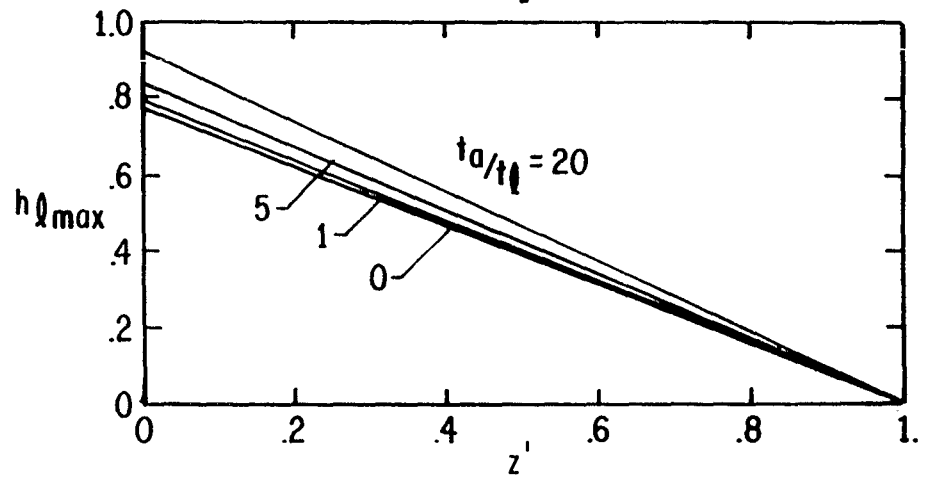
A. VALUE OF MAXIMUM VS.  $z'$  WITH  $t_a/t_q$  AS A PARAMETER:  
 $t_o/t_q = 1$



B. VALUE OF MAXIMUM VS.  $z'$  WITH  $t_a/t_q$  AS A PARAMETER:  
 $t_o/t_q = 1$

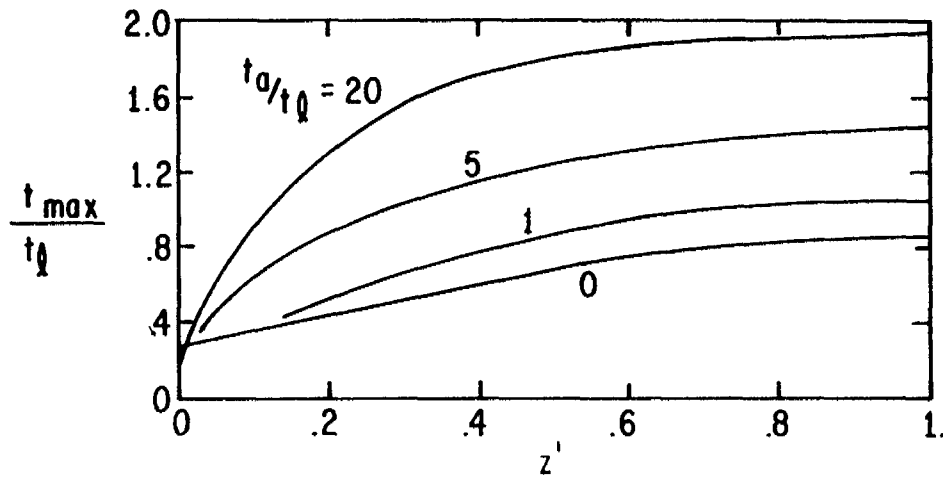


C. VALUE OF MAXIMUM VS  $z'$  WITH  $t_a/t_q$  AS A PARAMETER:  
 $t_o/t_q = 3$

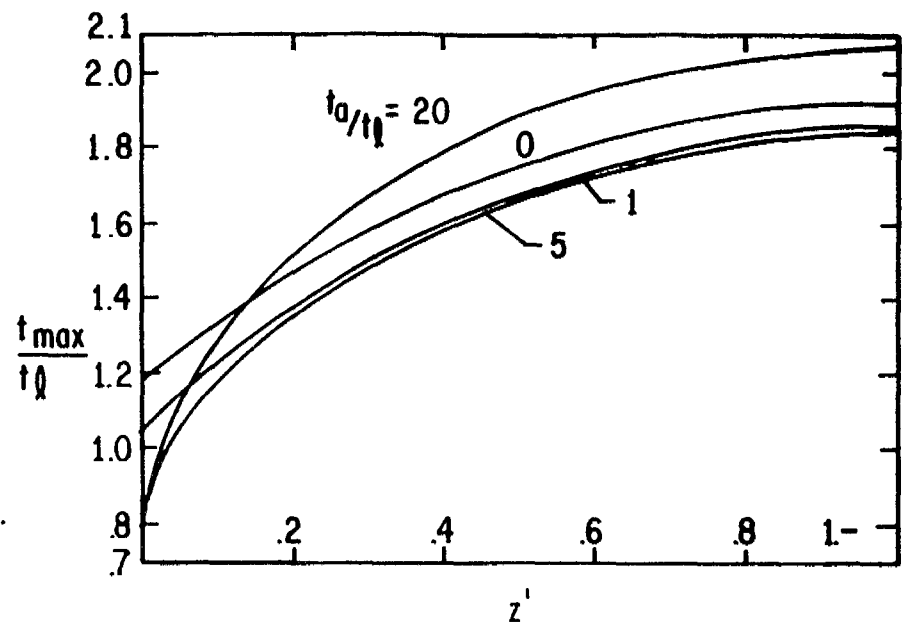


D. VALUE OF MAXIMUM VS  $z'$  WITH  $t_a/t_q$  AS A PARAMETER:  
 $t_o/t_q = 10$

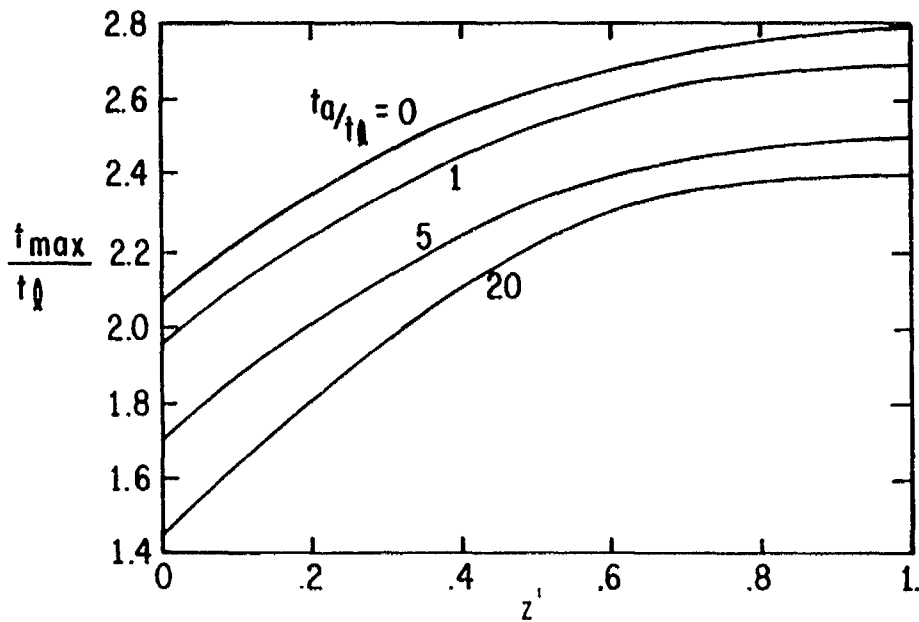
FIGURE 22. VALUE OF MAXIMUM OF CURRENT OR MAGNETIC FIELD PULSE SHAPE VS DEPTH IN GROUND FOR FINITE LENGTH TRANSMISSION LINE



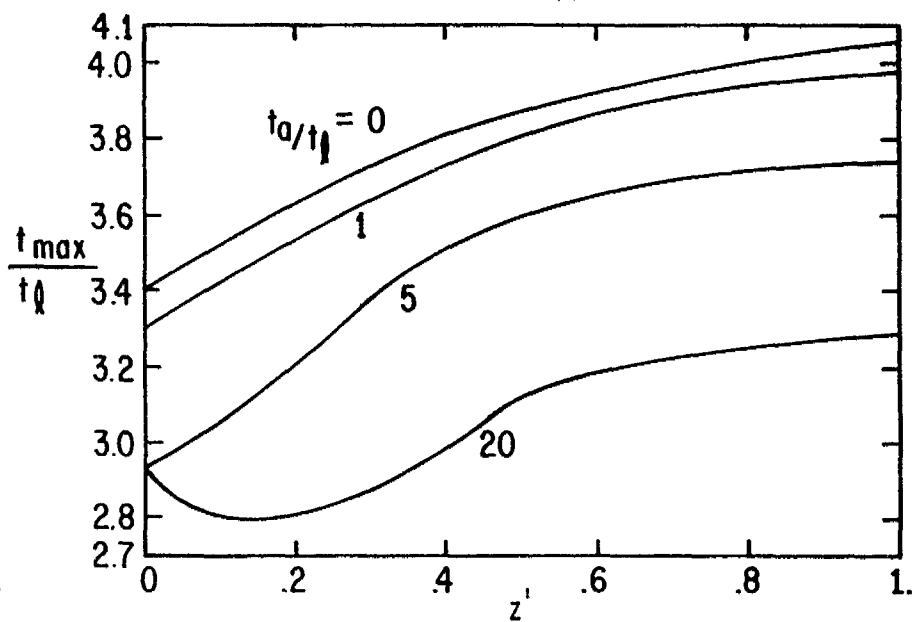
A. TIME OF MAXIMUM VS  $z'$  WITH  $t_0/t_q$  AS A PARAMETER:  $t_0/t_q = 1$



B. TIME OF MAXIMUM VS  $z'$  WITH  $t_0/t_0$  AS A PARAMETER:  $t_0/t_q = 1$

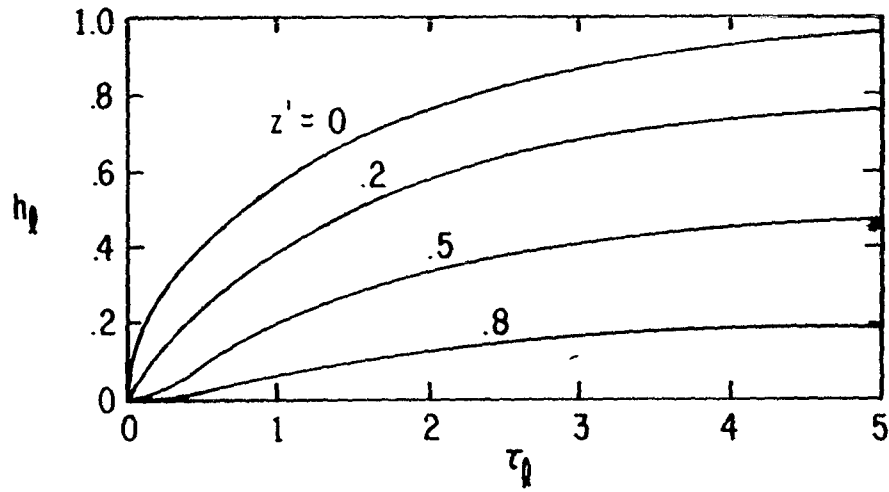


C. TIME OF MAXIMUM VS  $z'$  WITH  $t_0/t_q$  AS A PARAMETER:  $t_0/t_q = 3$

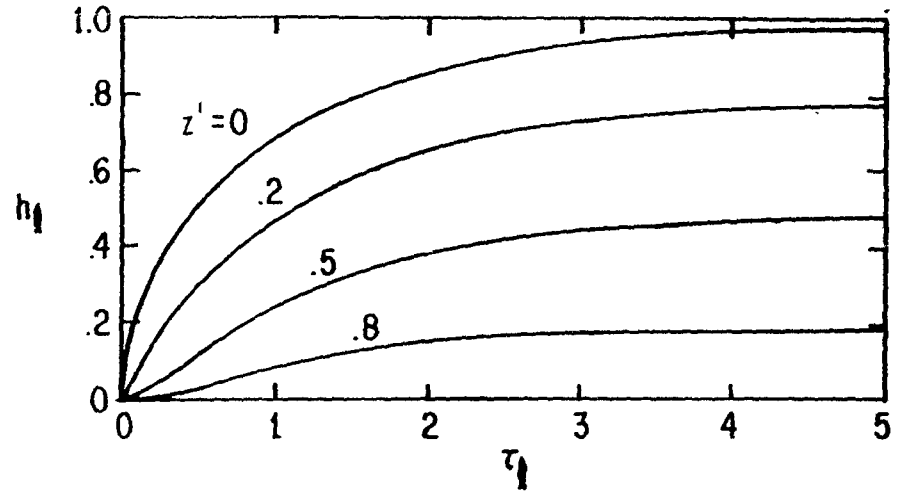


D. TIME OF MAXIMUM VS  $z'$  WITH  $t_0/t_q$  AS A PARAMETER:  $t_0/t_q = 10$

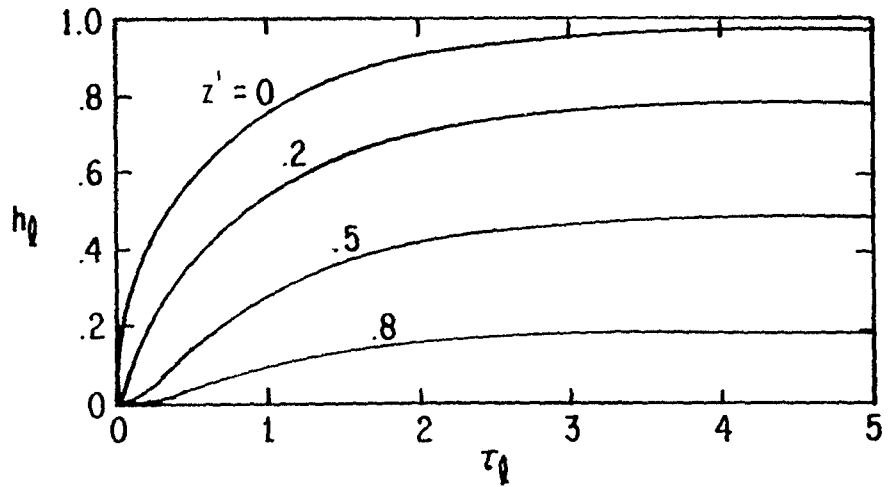
FIGURE 23: TIME OF MAXIMUM OF CURRENT OR MAGNETIC FIELD PULSE SHAPE VS DEPTH IN GROUND FOR FINITE LENGTH TRANSMISSION LINE



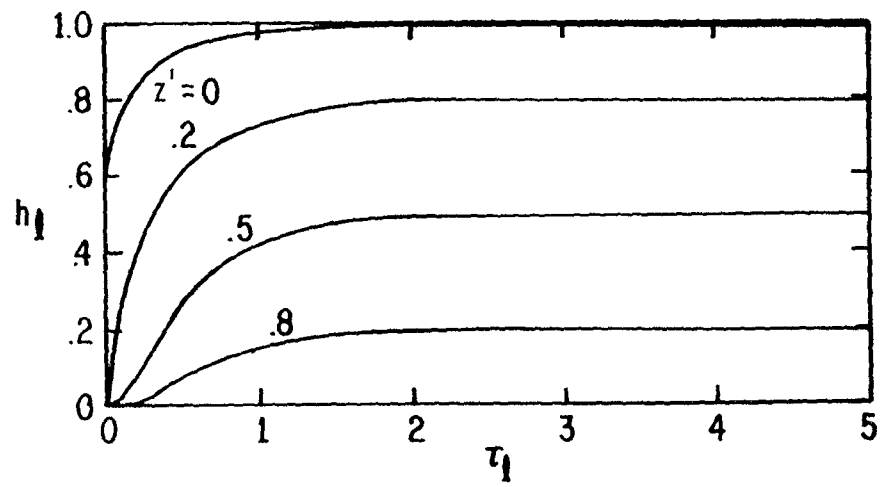
A.  $h_l$  vs  $\tau_l$  WITH  $z'$  AS A PARAMETER:  $R_a/R_0 = 0$



B.  $h_l$  vs  $\tau_l$  WITH  $z'$  AS A PARAMETER:  $R_a/R_0 = .5$

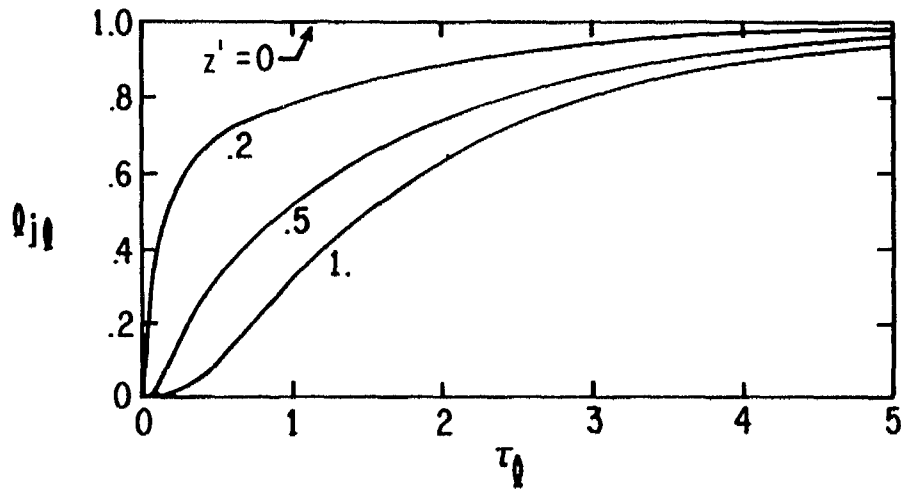


C.  $h_l$  vs  $\tau_l$  WITH  $z'$  AS A PARAMETER:  $R_a/R_0 = 1$

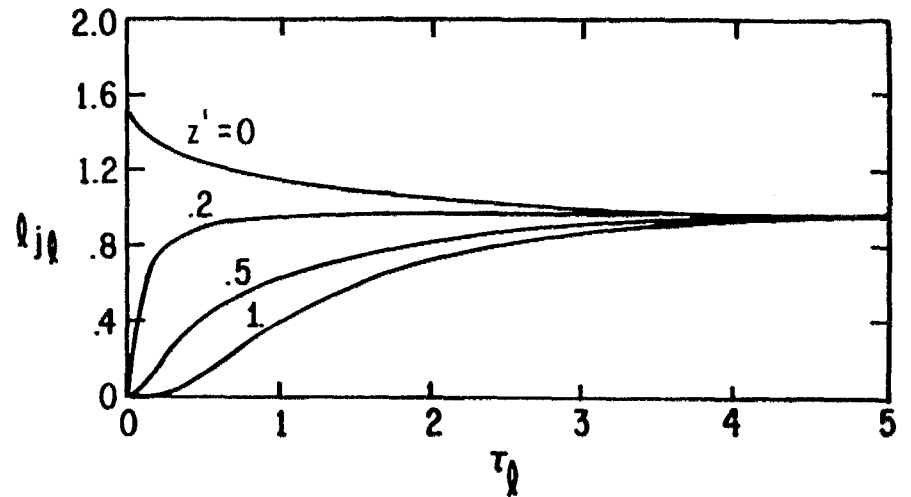


D.  $h_l$  vs  $\tau_l$  WITH  $z'$  AS A PARAMETER:  $R_a/R_0 = 10$

FIGURE 24. CURRENT OR MAGNETIC FIELD PULSE SHAPE FOR FINITE LENGTH TRANSMISSION LINE AND INFINITE GENERATOR CAPACITANCE

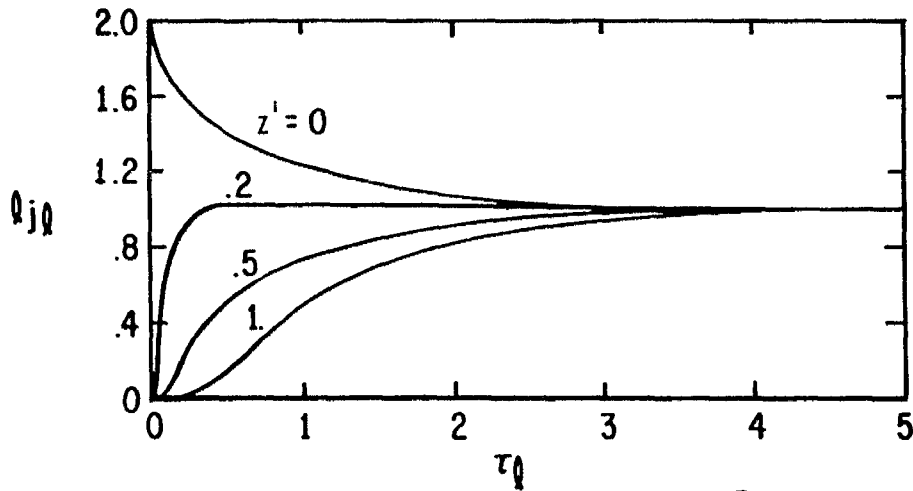


A.  $Q_{j(t)}$  vs  $\tau(t)$  WITH  $z'$  AS A PARAMETER:  $R_0/R_0 = 0$

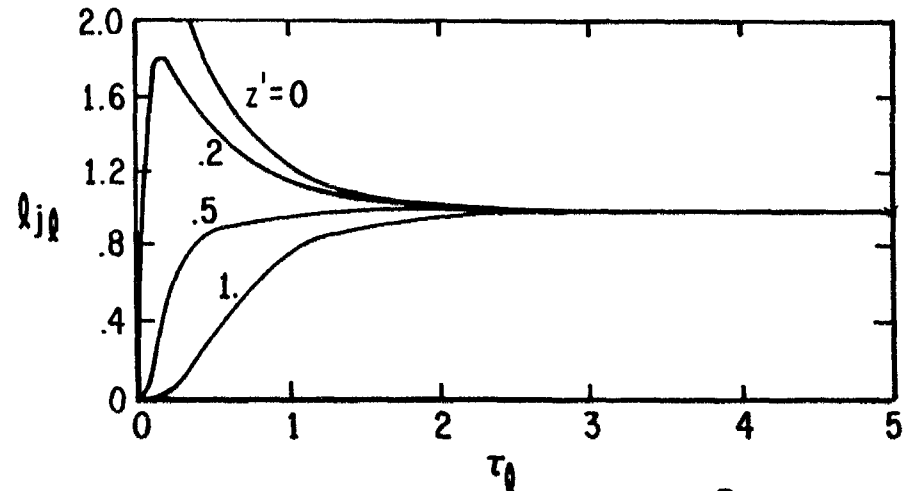


B.  $Q_{j(t)}$  vs  $\tau(t)$  WITH  $z'$  AS A PARAMETER:  $R_0/R_0 = .5$

07



C.  $Q_{j(t)}$  vs  $\tau(t)$  WITH  $z'$  AS A PARAMETER:  $R_0/R_0 = 1$



D.  $Q_{j(t)}$  vs  $\tau(t)$  WITH  $z'$  AS A PARAMETER:  $R_0/R_0 = 10$

FIGURE 25. VOLTAGE OR CURRENT DENSITY PULSE SHAPE FOR FINITE LENGTH TRANSMISSION LINE AND INFINITE GENERATOR CAPACITANCE

#### IV. Some Low-Frequency Considerations

While, in many cases, we do not have a convenient mathematical expression for the pulse shapes, there are some parameters of the pulses which can be simply expressed. In particular the complete time integral of the pulses can be found by using the final-value theorem of the Laplace transform. Beginning with the magnetic field pulse shape we have

$$\int_0^{\infty} h_{\ell}(\tau_{\ell}) d\tau_{\ell} = \lim_{s_{\ell} \rightarrow 0} s_{\ell} \left[ \frac{\tilde{h}_{\ell}(s_{\ell})}{s_{\ell}} \right] = \lim_{s_{\ell} \rightarrow 0} \tilde{h}_{\ell}(s_{\ell}) \quad (59)$$

Note that  $\tilde{h}_{\ell}(s_{\ell})/s_{\ell}$  is the normalized Laplace transform of the time integral of  $h_{\ell}(\tau_{\ell})$ . Then using equation (51) for  $h_{\ell}(s_{\ell})$  gives

$$\int_0^{\infty} h_{\ell}(\tau_{\ell}) d\tau_{\ell} = (1-z) \frac{t_0}{t_{\ell}} \left[ 1 + \frac{t_a}{t_0} \right] = (1-z) \left[ \frac{t_0}{t_{\ell}} + \frac{t_a}{t_{\ell}} \right] \quad (60)$$

Using equation (54) for the normalized current density pulse shape gives

$$\int_0^{\infty} j_{\ell}(\tau_{\ell}) d\tau_{\ell} = \lim_{s_{\ell} \rightarrow 0} j_{\ell}^{\sim}(s_{\ell}) = \frac{t_0}{t_{\ell}} + \frac{t_a}{t_{\ell}} \quad (61)$$

Thus the time integral of the current density pulse is conserved with depth while the time integral of the magnetic field pulse falls off with depth as  $1-z'$ .

Up until this point we have only considered the case of uniform ground conductivity. However, the complete time integral of the pulse shapes only involves the case of  $s_{\ell}=0$  or zero frequency. The variation of the time integral of the pulses with depth can then be considered without much complication for non-uniform ground conductivity. In particular, allow  $\sigma$  to be a function of  $z'$  but not a function of  $x$  or  $y$ . Consider first the current density. The voltage on the transmission line is uniform with depth at zero frequency, and thus the electric field is also uniform with depth at zero frequency. However, the current density is proportional to the conductivity. Thus we generalize the complete time integral of the normalized current density as

$$\int_0^{\infty} j_{\ell}(\tau_{\ell}) d\tau_{\ell} = \frac{\sigma(z)}{\sigma_{\text{avg}}} \left[ \frac{t_0}{t_{\ell}} + \frac{t_a}{t_{\ell}} \right] \quad (62)$$

where

$$\sigma_{\text{avg}} = \int_0^1 \sigma(z) dz \quad (63)$$

We also have to redefine

$$R_0 \equiv \frac{f_g}{l\sigma_{avg}} \quad (64)$$

and

$$t_l \equiv \frac{\mu\sigma_{avg} l^2}{4} \quad (65)$$

for these parameters to have meaning for the case of  $\sigma$  varying with depth. Note that equation (62) reduces to equation (61) if  $\sigma$  is independent of  $z'$ . For  $\sigma$  a function of  $z'$ , however, the complete time integral of the normalized current density is proportional to  $\sigma(z')$ .

Now consider the time integral of the normalized magnetic field for  $\sigma$  a function of  $z'$ . The current on the transmission line at a given depth and the magnetic field at that depth are proportional to the integral of the current density from the bottom of the transmission line up to that depth. The current density is in turn proportional to the conductivity. Thus we generalize the complete time integral of the normalized magnetic field as

$$\int_0^{\infty} h_l(\tau_l) d\tau_l = \left[ \frac{t_0}{t_l} + \frac{t_a}{t_l} \right] \frac{1}{\sigma_{avg}} \int_{z'}^l \sigma(z'') dz'' \quad (66)$$

This reduces to equation (60) if  $\sigma$  is independent of  $z'$ . If  $\sigma$  is a function of  $z'$ , however, the complete time integral of the magnetic field has a somewhat more complicated dependence on depth.

## V. Summary

We have calculated the pulse shapes of the electromagnetic field components on the buried transmission line for a capacitive generator with a series resistance. There are various idealizing assumptions used: The ground conductivity is assumed uniform with depth and independent of frequency. Frequencies of interest are assumed low enough that the ground permittivity and the transit time over the ground surface may be neglected in the calculations. Extra impedances associated with the generator and the transition structure to the transmission line are also neglected.

There is a characteristic diffusion time,  $t_d$ , for the buried transmission line and the calculations consider two cases. First, times of interest in the pulse are small compared to  $t_d$  and the length of the transmission line is assumed infinite for the calculations. Second, times of interest are of the order of or larger than  $t_d$  and the length of the transmission line is included. Depending on the values of the various parameters of the generator and the transmission line, the pulse shapes of the electromagnetic field components may oscillate. In such a case if one desires he may increase the damping resistance until the oscillation is removed. The damping resistance may also be increased in order to broaden the magnetic field pulse and decrease its rise time, but at the expense of amplitude. There are other types of impedances which one might add at the top of the transmission line to further shape the electromagnetic field pulses but such impedances are not considered in this note.

A computer code was used to numerically calculate the inverse Fourier transforms (reference 2) The indicated relative errors in the pulse shapes are at worst about .03, and generally are much smaller than that. In converting the Laplace transforms to Fourier transforms difficulty was encountered at  $\omega=0$  for cases in which the time domain pulses had infinite time integrals. This difficulty was removed by slightly altering the Fourier transforms so that the area of the time domain pulses remained finite. The distortion was made to occur at times much greater than those used for the plots and the errors so introduced at times of interest were kept as small as those associated with the numerical inverse transform.